KOPIO signal and backgrounds

1. Backgrounds considered
2. Tools (measurements and simulation)
3. Veto and resolution assumptions
4. Flux assumptions
5. Detection methods
6. Background mechanisms
7. Background from $\mathbf{K_L^0}$ decays
8. Event selection: technique and results
9. Background not from $\mathbf{K_L^0}$ decays
10. $\boldsymbol{\mathcal{B}}(\mathbf{K_L^0} \rightarrow \boldsymbol{\pi^0 \nu \bar{\nu}})$ precision and sensitivity

Signal and K_L^0 backgrounds considered

Name	Final state	Branching fraction	$\mathcal{B}/\mathcal{B}(K_L^0 \to \pi^0\nu\bar{\nu})$
Kpnn	$\pi^0\nu\bar{\nu}$	0.3000×10^{-10}	1.000
Kp2	$\pi^0\pi^0$	0.9320×10^{-3}	0.31×10^{8}
Kp3	$\pi^0\pi^0\pi^0$	0.2105	0.70×10^{10}
Kcp3	$\pi^+\pi^-\pi^0$	0.1259	0.42×10^{10}
Ke3g	$\pi^\pm e^\mp\nu\gamma$	0.3530×10^{-2}	0.12×10^{9}
Ke4	$\pi^0\pi^\pm e^\mp\nu$	0.5180×10^{-4}	0.17×10^{7}
Kcp2	$\pi^+\pi^-$	0.2090×10^{-2}	0.70×10^{8}
Kgg	$\gamma\gamma$	0.5900×10^{-3}	0.20×10^{8}
Ke3	$\pi^\pm e^\mp\nu$	0.3881	0.13×10^{11}
Km3	$\pi^\pm \mu^\mp\nu$	0.2719	0.91×10^{10}
Km3g	$\pi^\pm \mu^\mp\nu\gamma$	0.5700×10^{-3}	0.19×10^{8}
Kpgg	$\pi^0\gamma\gamma$	0.1410×10^{-5}	0.47×10^{5}
Km4	$\pi^0\pi^\pm\mu^\mp\nu$	0.1400×10^{-4}	0.47×10^{6}
Ke2g	$e^+e^-\gamma$	0.1000×10^{-4}	0.33×10^{6}
Km2g	$\mu^+\mu^-\gamma$	0.3590×10^{-6}	0.12×10^{5}
Kbet	$K^\pm e^\mp\nu$	0.1080×10^{-7}	360

Non-K_L^0 backgrounds considered

- Hyperons, primarily $\Lambda \to \pi^0 n$
- K_S^0
- $K^\pm$ contamination of beam
- $\pi^\pm \to \pi^0 e^\pm \nu$
- $nN \to \pi^0 X$
- $\bar{n}N \to \pi^0 X$
- Fake photons
- Two K_L^0 giving a single candidate

Tools

- FastMC: “Fast” simulation of KOPIO with simple geometry and parametrized responses based on measurements and/or more detailed simulation. Main tool for estimating signal and background acceptances and yields.
- GEANT3.21: Primarily used to estimate trigger, reconstruction efficiencies and to estimate signal losses due to stopped muon decays, neutron interactions, self-vetoing and vetoing by other $\mathbf{K_L^0}$ in a microbunch. Also used to estimate secondary $\mathbf{K_L^0}$ production in target and $\mathbf{K_L^0}$ attenuation in spoiler.
- FLUKA, GEANT4 : Investigate effect of photonuclear interactions on photon veto (PV) inefficiency.
- MCPNX : Neutron propagation and interaction
- KOPTICS, GEANT4 : ray-tracing optics in scintillator, scintillation processes.
- SLEX-LONG1D : Beam microbunch simulation

FastMC features

- $\mathbf{K_L^0}$ and neutron beam momentum, angular dependence from measurements
- Extended target
- Time-structure of incident proton beam
- All $\mathbf{K_L^0}$ $\pi^{\pm}$, $\mu^{\pm}$, π^0 decay modes. Decay-in-flight.
- No magnetic fields
- Preradiator(PR) and calorimeter(CAL) response parametrized from measurements
- Hermeticity assumed (except for tracks exitting decay volume via beam entrance hole).
- Photon veto (PV) inefficiency as a function of energy and incidence angle parametrized from measurement and simulation for the main photon veto and for the beam catcher
- Charged particle veto (CV) inefficiency as a function of species and momentum parametrized from measurements

FastMC photon veto parametrizations

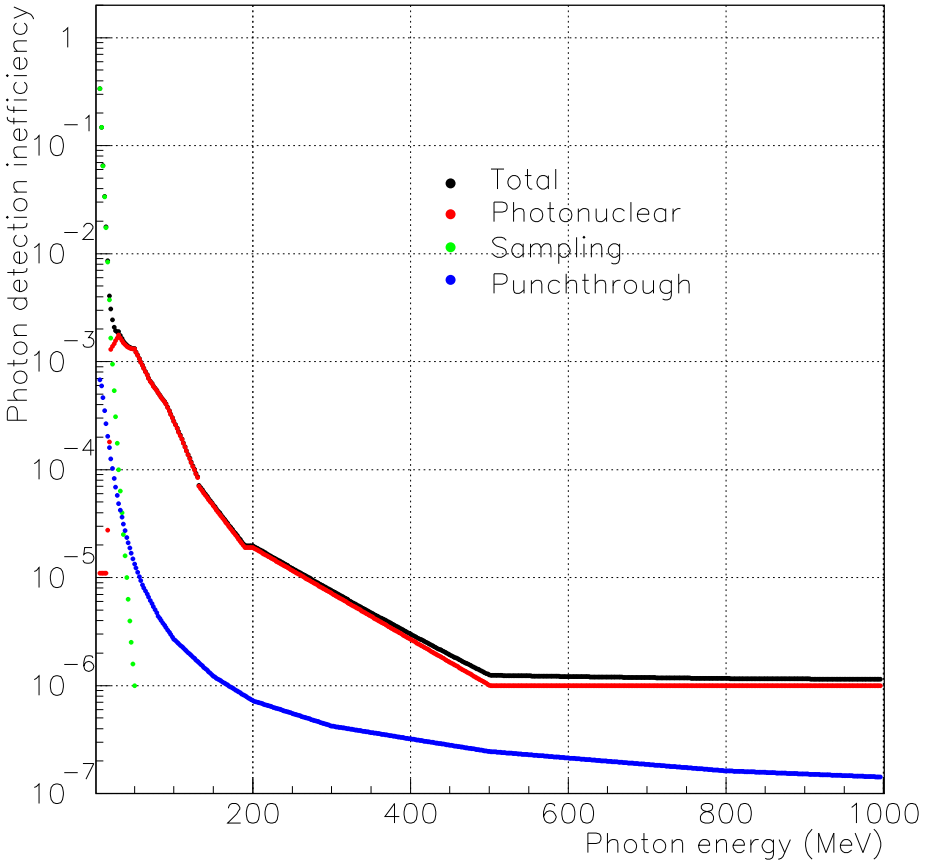

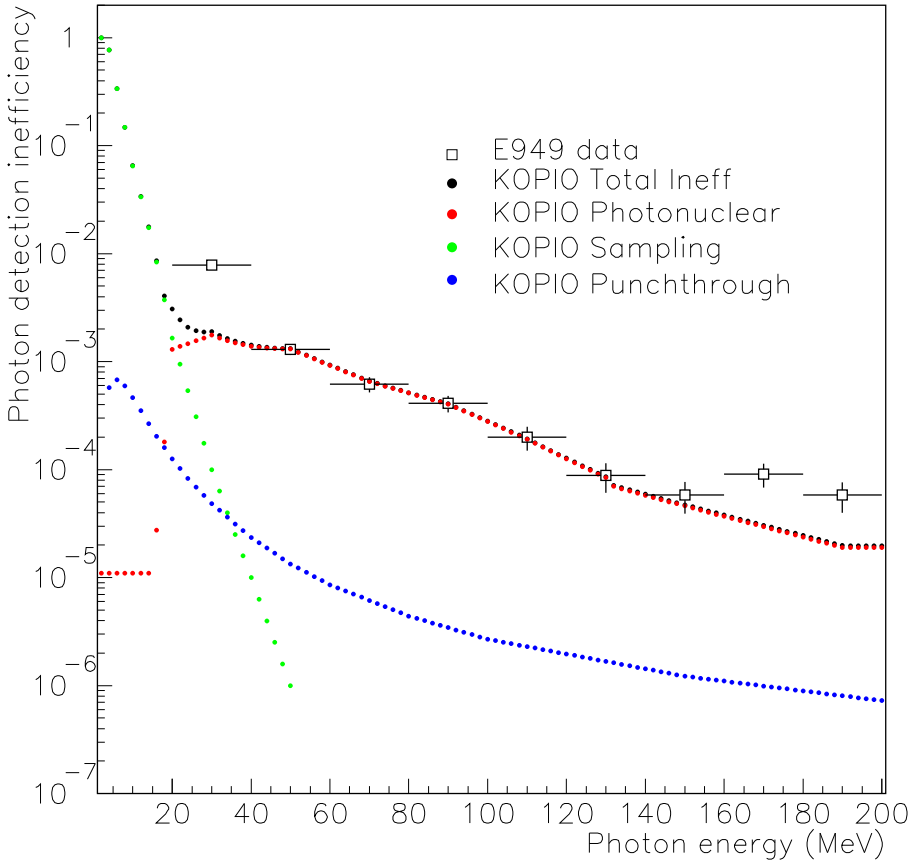

FastMC beam catcher PV parametrization

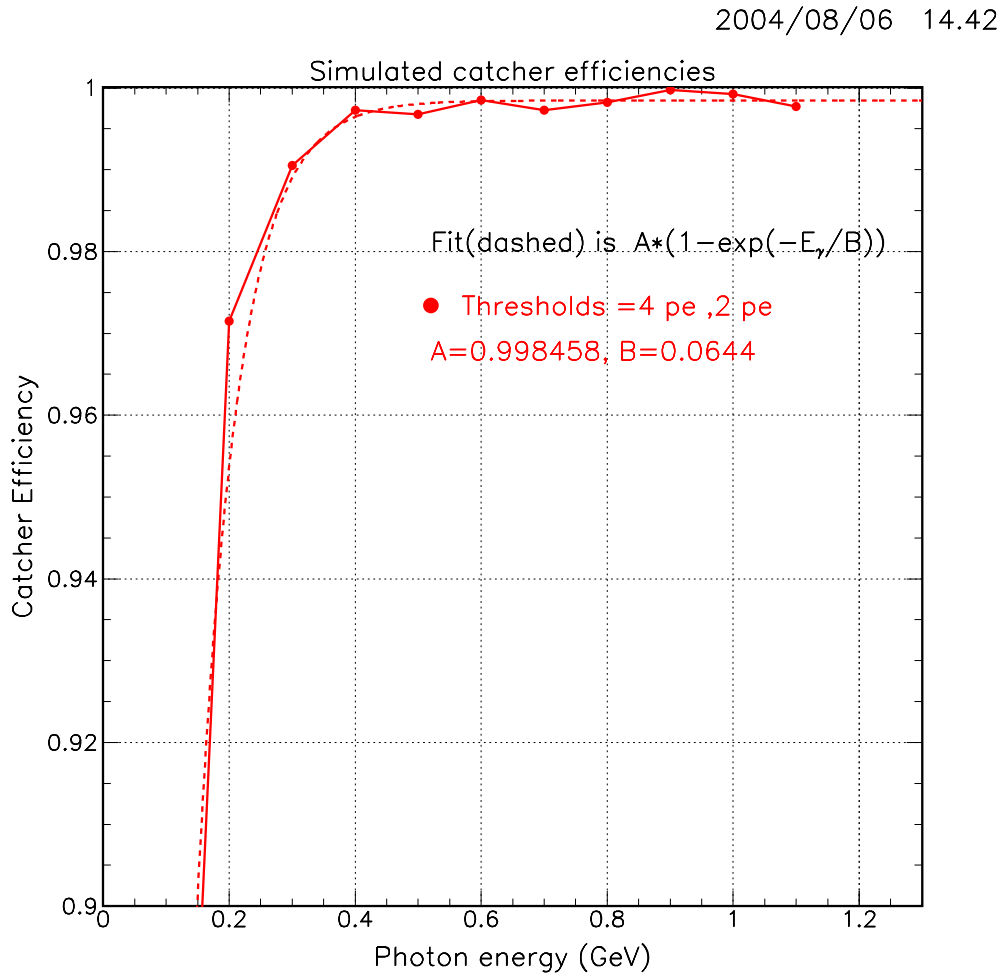

FastMC charged pion veto parametrizations

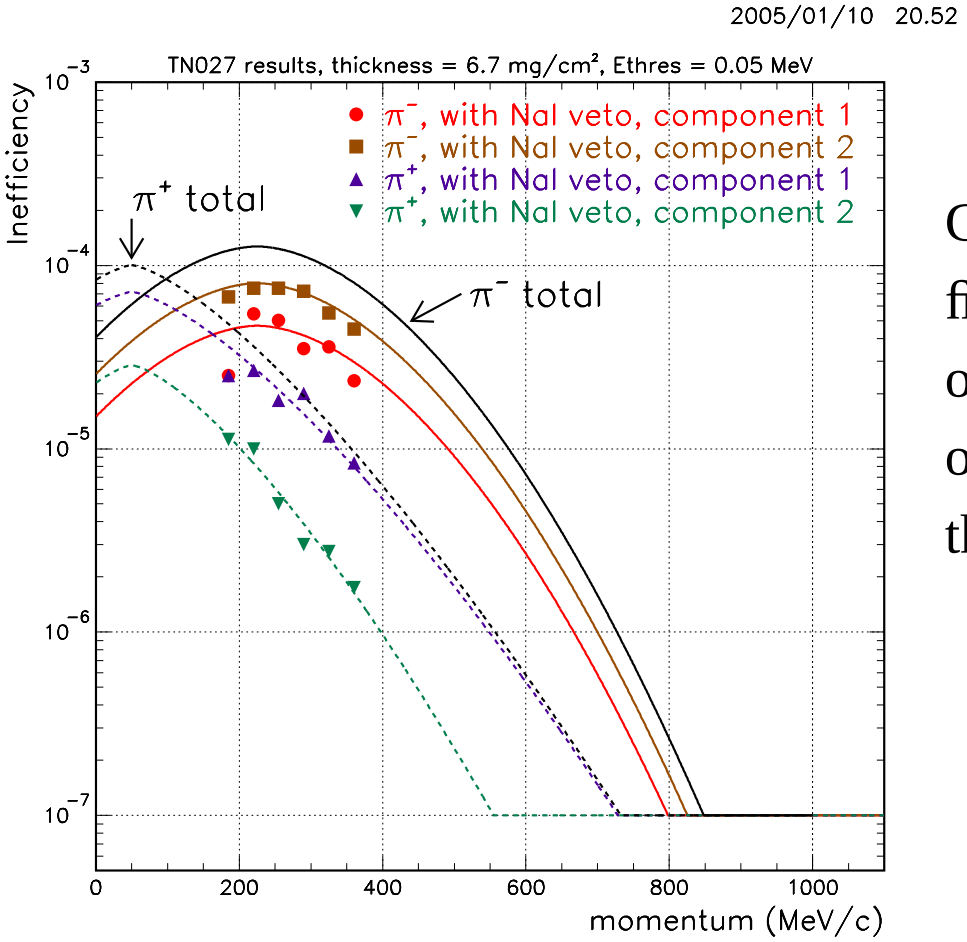

Charged pion inefficiencies taken from fits to PSI measurements and extrapolated for a dead material thickness of 6.7 mg/cm^2 and a 50 keV energy threshold.

Component 1	Dead material
Component 2	Threshold

FastMC $\mu^{\pm}$, $e^{\pm}$ veto parametrizations

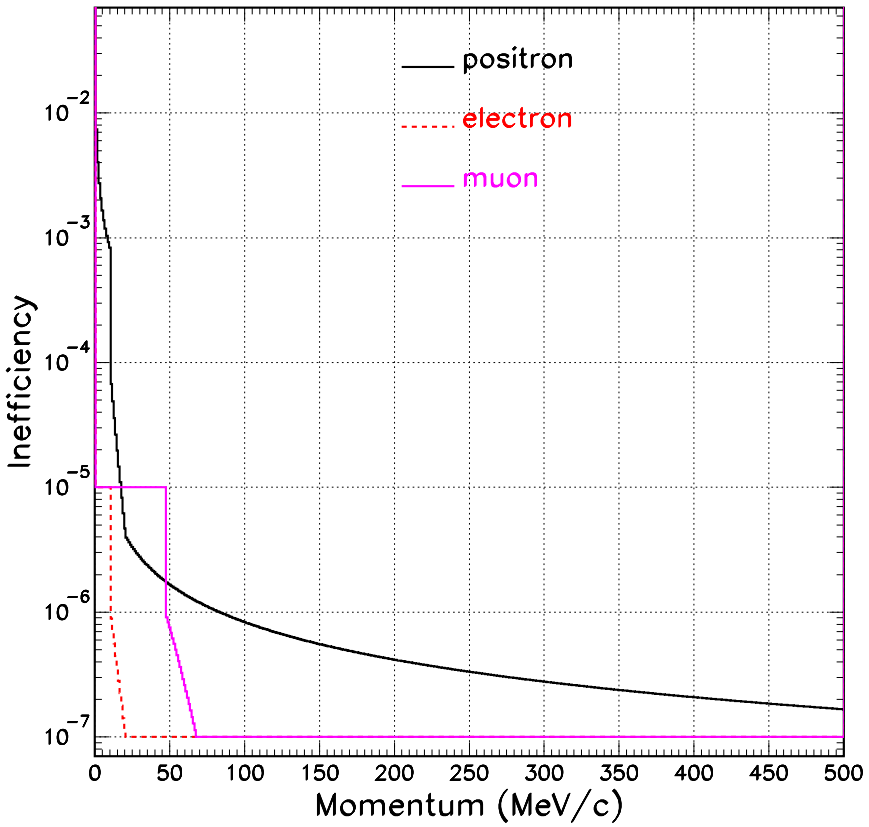

Positron inefficiency from approximation to annihilation cross-section. All inefficiencies reduced by up to $\times \mathbf{0.01}$ due to detection by PV behind all CV elements.

Photon energy, angle and position measurement assumptions

- Energy resolution : $\mathbf{2.7\%/\sqrt{E(GeV)}}$
- Time resolution : $\mathbf{90\ ps/\sqrt{E(GeV)}}$
- PR angular resolution is parametrized as double gaussian as a function of photon incident angle and energy (Figure)
- PR position resolution : $\mathbf{0.02\ cm}$
- Shashlyk position resolution :
  - Longitudinal 1.5cm (corresponds to 50 ps)
  - Transverse
    - CAL 3.17 cm (11cm/$\sqrt{\mathbf{12}}$)
    - Barrel Veto (BV) 6.34 cm (22cm /$\sqrt{\mathbf{12}}$)

PR angular resolution

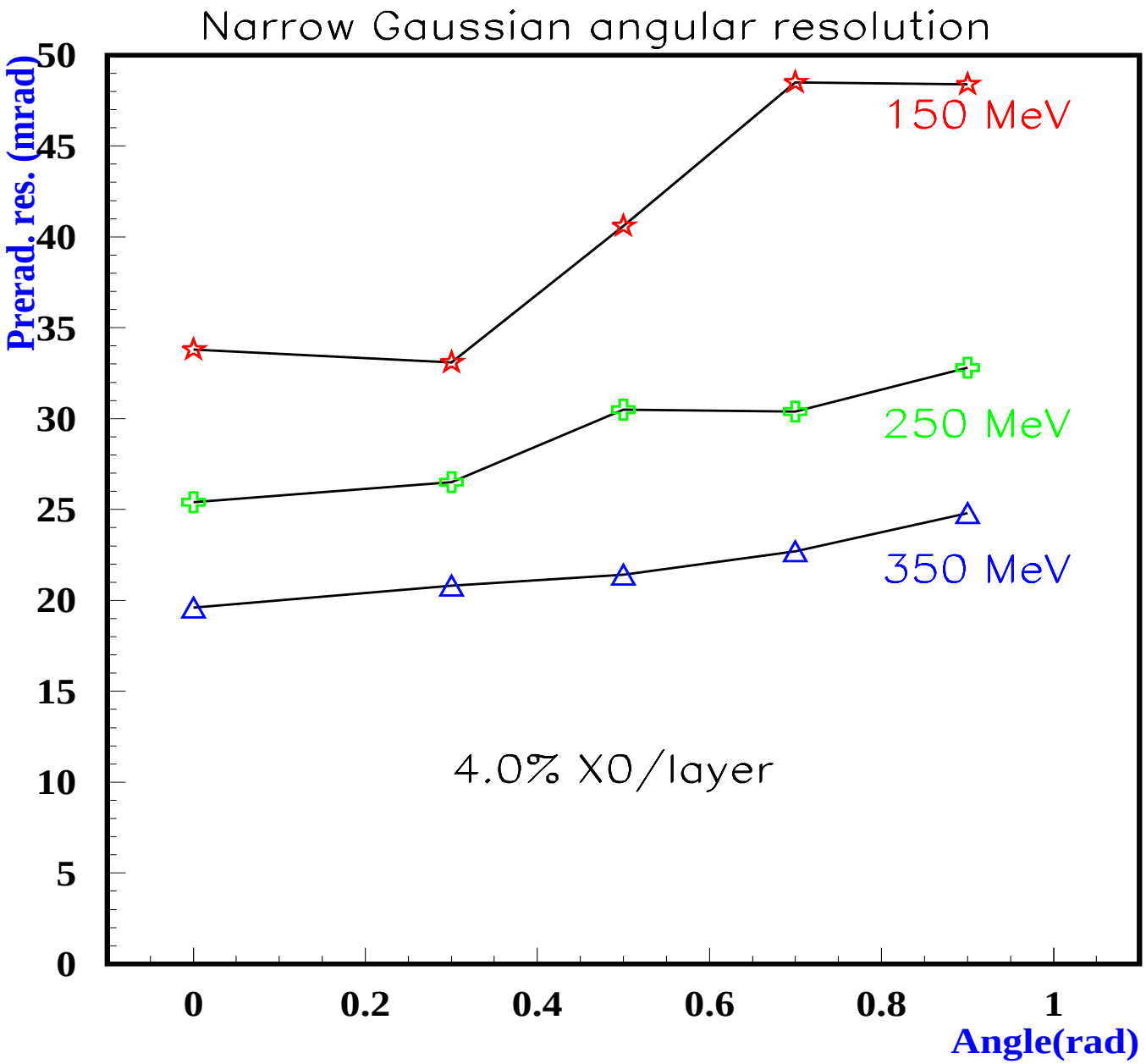

FastMC kinematic fitter

Two sequential kinematic fits are attempted for every pair of photon candidates using a non-linear least-squares fitter with constraints. The first fit does not impose the π^0 mass constraint, and the second fit does impose the mass constraint. The constraint of the y-beam envelope is imposed in both fits.

The reconstructed production vertex of the π^0 (and $\mathbf{K_L^0}$) is required to produce a physically meaningful value of β when the $\mathbf{K_L^0}$ production point is assumed to be at the center of the target at t=0.

Flux assumptions

$\mathbf{42.5^\circ}$	production angle
$\mathbf{90 \times 4\ mrad^2}$	aspect ratio
25.5 GeV/c	proton beam momentum
100TP	protons/spill (TP$\equiv \mathbf{10^{12}}$protons)
25MHz	microbunch frequency
2.3s	interspill length
5.2s	spill length †
2.1	average number of $\mathbf{K^0_L}/\mu$bunch exitting spoiler
12000	Hours of running
0.378	$\mathbf{K^0_L}$ survival factor
$\mathbf{1.33 \times 10^7}$	Useful $\mathbf{K^0_L}$ decays exiting spoiler/calendar-second

Useful $\mathbf{K^0_L}$ decays exitting spoiler/calendar-second takes into account all assumed losses ("$\mathbf{K^0_L}$ survival factor").

† The optimum spill length may change as knowledge of expected random rates, achievable pulse pair resolution and other parameters improves. The sensitivity is a shallow function of the spill length near the optimum value (next page).

KOPIO sensitivity *vs* spill length

The relative KOPIO sensitivity as a function of spill length. The optimum spill length is 5.2 seconds; however, spill lengths from ~ 4 to ~ 7 seconds would entail only a $\sim 5\%$ sensitivity loss.

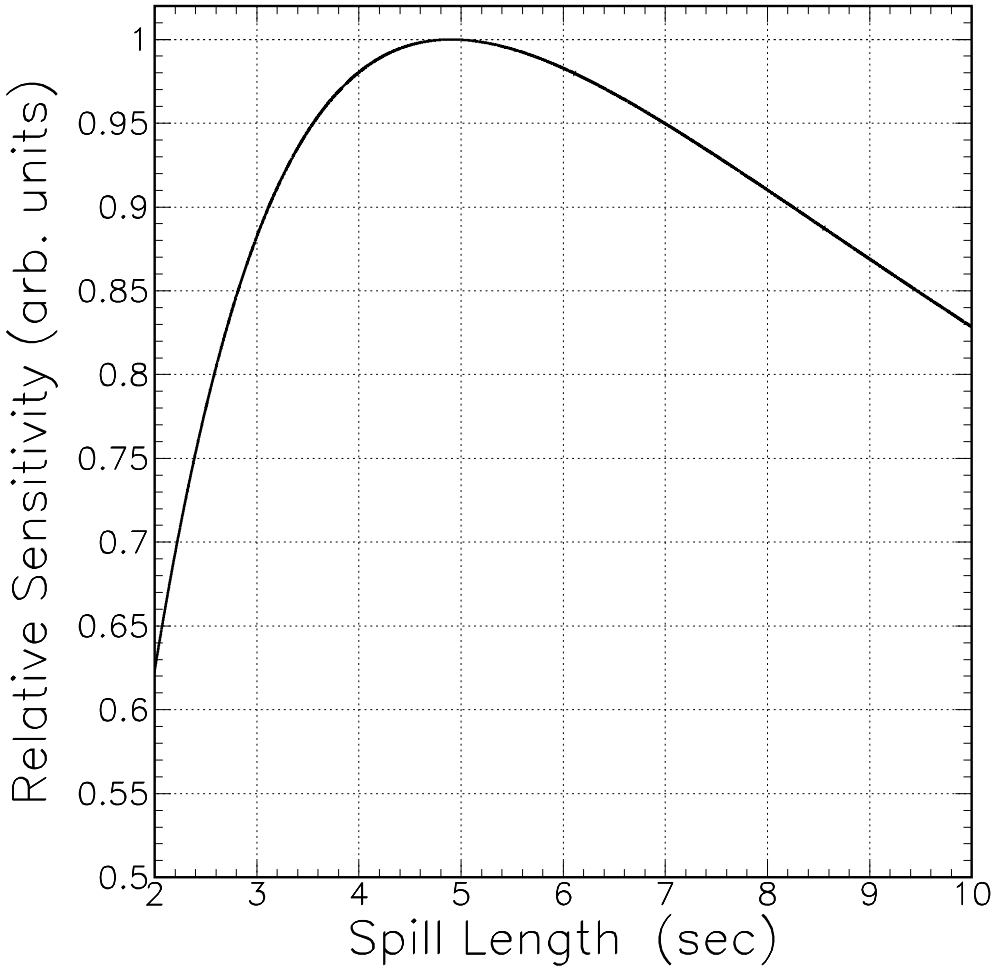

Signal losses used in spill length optimization

Losses include an estimated range of uncertainty.

- Independent of instantaneous rate

$\mathbf{0.88^{+0.05}_{-0.10}}$	Self-veto
$\mathbf{0.86^{+0.04}_{-0.02}}$	Photon absorption in vacuum vessel

- Rate dependent (veto rates assume optimal spill length)

$\mathbf{0.62 \pm 0.02}$	Vetoing by other $\mathbf{K^0_L}$ in the same microbunch
$\mathbf{0.885 \pm 0.013}$	Vetoing by stopped muon decays
$\mathbf{0.978 \pm 0.002}$	Vetoing by $\mathbf{K^0_L}$ in adjacent microbunch
$\mathbf{0.986 \pm 0.010}$	Vetoing by halo neutrons
$\mathbf{0.956 \pm 0.002}$	Vetoing by neutrons in catcher
$\mathbf{0.982 \pm 0.002}$	Vetoing by $\mathbf{K^0_L}$ in catcher

Overall $\mathbf{K^0_L}$ survival rate at optimal spill length of 5.2s is 0.38 (including rate-independent factors).

Detection methods considered

1	**2**γPR/CAL	both γ convert in PR, energy in PR & CAL
2	**2**γPR/CAL+OV	both γ convert in PR, energy in PR,CAL & OV
3	**1**γPR/**1**γCAL	1 γ converts in CAL, 1 in CAL, energy in PR& CAL
4	**1**γPR/**1**γOV	1 γ converts in CAL, 1 in OV, energy in PR& OV
5	**1**γPR/**1**γBV	1 γ converts in CAL, 1 in BV, energy in PR& BV

Results will be shown for detection methods 2, 3 and 5.

"**2**γPR" = Method 2

"**1**γPR" = Methods 3 and 5

Method 1 (**2**γPR/CAL) is subsumed by method 2 (**2**γPR/CAL+OV) and the acceptance of method 4 (**1**γPR/**1**γOV) is very small.

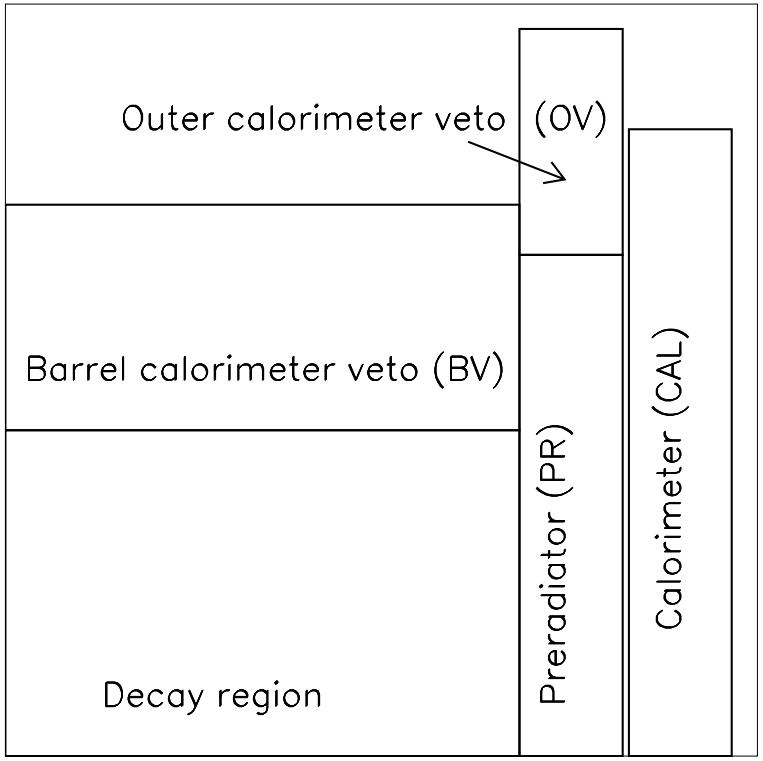

Background mechanisms

Each $\mathbf{K_L^0}$ decay mode is considered under the following mechanisms that can produce non-signal $\mathbf{K_L^0} \longrightarrow \boldsymbol{\pi^0 \nu \bar{\nu}}$ candidates.

1. "standard" : $\mathbf{K_L^0}$ decays within microbunch
2. interbunch : $\mathbf{K_L^0}$ decays from interbunch $\mathbf{K_L^0}$ production
3. wrap-around : $\mathbf{K_L^0}$ from previous microbunch
4. accidental photons : $\mathbf{K_L^0}$ decay products combined with "fake" photons from stopped muon decays or neutron-induced showers
5. merged photons : $\boldsymbol{\pi^0}$ candidates from $\boldsymbol{\gamma}$ pairs that are too close to resolve spatially and temporally

"Fake" photon samples generated with GEANT3 and inserted into FastMC.

Merge criteria : $|\vec{x_1} - \vec{x_2}| < 5R_M$, $R_M = 5.98$ cm, $|\Delta t_{\gamma\gamma}| < 15ns$ (CAL APD double-pulse resolution)

Main K_L^0 decay mode backgrounds

Final state	Abbreviation	Branching fraction
$\pi^0\pi^0$	kp2	9.32×10^{-4}
$\pi^+\pi^-\pi^0$	kcp3	12.59%
$\pi^\pm e^\mp \nu\gamma$	ke3g	3.53×10^{-3}
$\pi^0\pi^\pm e^\mp \nu$	ke4	5.18×10^{-5}
$\pi^0\pi^0\pi^0$	kp3	21.05%

Signal	Abbreviation	SM branching fraction
$\pi^0\nu\bar{\nu}$	kpnn	3×10^{-11}

Rates from other K_L^0 decays are negligible (< 0.1 events/Total K_L^0 flux).

Nomenclature: kp2-even (kp2-odd) refers to case when photon candidates come from the same (different) π^0 .

Event selection criteria - Summary of technique

Apply "setup" cuts, ideally with high signal acceptance, designed to suppress non-$\mathbf{K_L^0}$ background and $\mathbf{K_L^0}$ background due to veto timing considerations.

For these 3 variables,

1. $\boldsymbol{M(\gamma\gamma) - M(\pi^0)}$: $\boldsymbol{M(\gamma\gamma)}$ is the fitted $\boldsymbol{\pi^0}$ candidate mass
2. $\boldsymbol{T^{*2}}$: $\boldsymbol{T^*}$ is the kinetic energy of the $\boldsymbol{\pi^0}$ candidate in the $\mathbf{K_L^0}$ CMS
3. $\boldsymbol{\ln(E_{miss})}$: $\boldsymbol{E_{miss} \equiv E(K_L^0) - E(\pi^0)}$ is the lab missing energy (MeV)

Use a 3-dimensional binned 'likelihood' method to maximize signal/background (S/B) for a given signal rate.

1. For each bin defined by the above three variables: Add up all backgrounds. Add up signal. Calculate S/B.
2. Sort bins by decreasing S/B; integrate S & B according to order of sort.
3. Define specific realizations of the general cut by noting when integrated S crosses various arbitrary thresholds.

2005/01/09 00.56

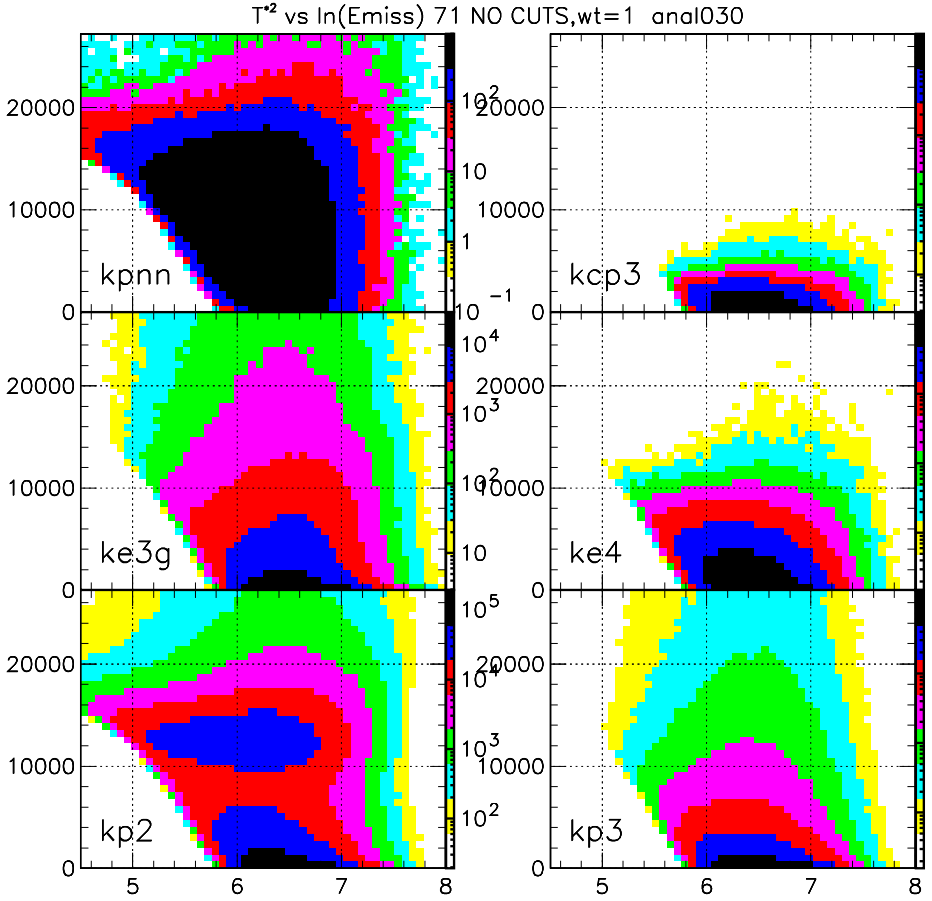

T^{*2} *vs* $\ln(E_{\mathrm{miss}})$

2005/01/09 00.59

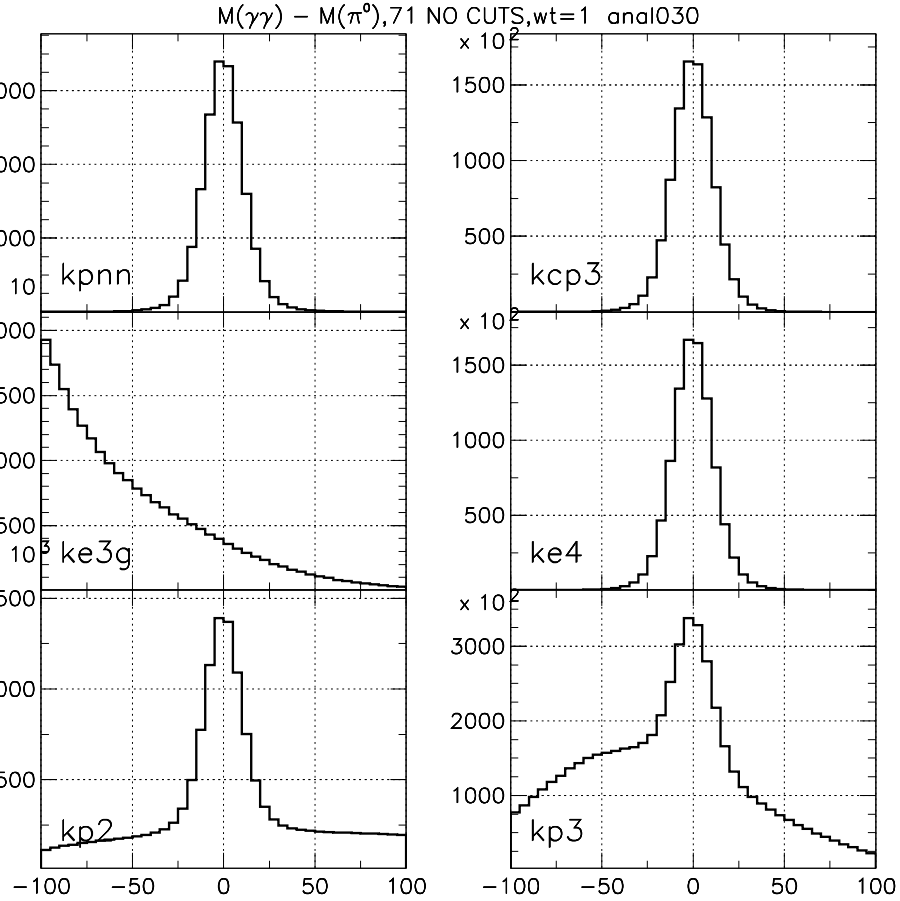

$M(\gamma,\gamma) - M(\pi^0)$

"Setup" cuts

Cut	Comment
$\chi^2 < 100$	Reasonable kinematic fit
$DOCA < 60$ cm	Suppress non- $\mathbf{K^0_L}$ backgrounds
$z_1 < z(\mathbf{K^0_L}) < z_2$	Suppress neutron-induced background
$P(\mathbf{K^0_L}) > 400\ \mathbf{MeV}/c$	Suppress $\mathbf{K^0_L}$ background from next microbunch
$M^2_\nu < -30000\ (\mathbf{MeV}/c^2)^2$	Suppress background involving slow charged tracks
$\mathbf{DK12 < 30\ cm}$	Suppress background involving mis-recon. $z(\mathbf{K^0_L})$
$-30 < M_{\gamma\gamma} - M_{\pi^0} < 40\ \mathbf{MeV}$	Suppress background when $\gamma\gamma$ not from a single π
$E^*_{\pi^0} < 300\ \mathbf{MeV}$	Suppress non-$\mathbf{K^0_L}$ backgrounds

DOCA = Distance Of Closest Approach of 2 candidate γ

$z(\mathbf{K^0_L})$ = reconstructed z of $\mathbf{K^0_L}$ candidate

z_1 is 75cm (100cm) from US end of decay volume for $\mathbf{2}\gamma$PR ($\mathbf{1}\gamma$PR)

z_2 is 50cm (100cm) from DS end of decay volume for $\mathbf{2}\gamma$PR ($\mathbf{1}\gamma$PR)

Suppressing background involving slow charged tracks

Define

$$\Delta \equiv t_{\rm hit} - t_{\rm K_L^0} - |\vec{x}_{\rm hit} - \vec{x}_{\rm K_L^0}|/c$$

where $t_{\rm hit}, \vec{x}_{\rm hit}$ are the time and position of veto hit, and $t_{\rm K_L^0}, \vec{x}_{\rm K_L^0}$ are the reconstructed time and position of the $\rm K_L^0$ decay.

With no bias in reconstructed $t_{\rm K_L^0}, \vec{x}_{\rm K_L^0}$, expect Δ to be symmetric about zero for γs and have a tail for $\Delta > 0$ due to slow charged tracks and decay-in-flight.

To suppress this tail, we require $M_\nu^2 < -30000\ ({\rm MeV}/c^2)^2$ and apply M_ν^2-dependent cut shown on next page, where
$M_\nu^2 \equiv (P({\rm K_L^0}) - P(\pi^0) - P(\pi))^2$ with $P(\pi) = M(\pi)$.

Note that $M_\nu^2 = M_K^2 + M_{\pi^0}^2 + M_\pi^2 - 2M_K E_{\pi^0}^* - 2M_\pi E_{\rm miss}$, so a cut on M_ν^2 is a straight line [curve] in the $E_{\pi^0}^*, E_{\rm miss}$ [$T^{*2}, \ln(E_{\rm miss})$] plane.

Suppressing background involving slow charged tracks

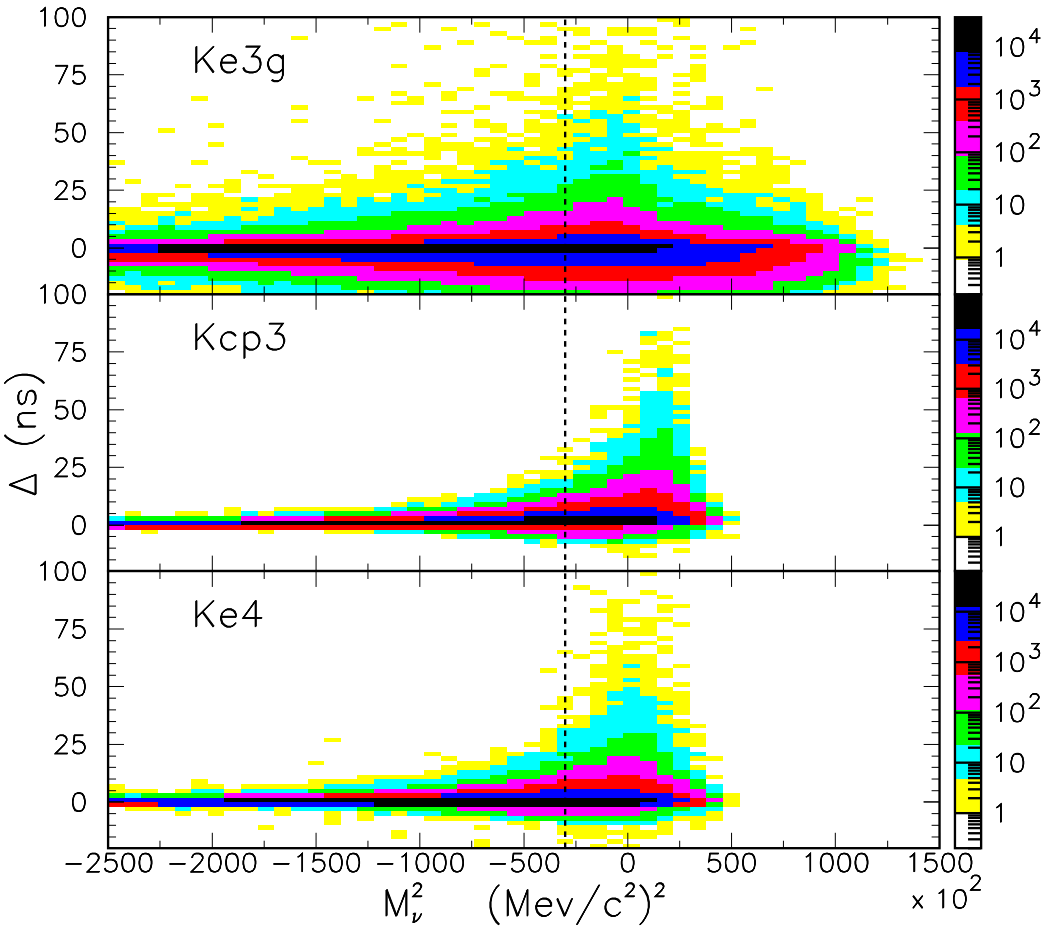

Δ vs M_ν^2 for $\pi^\pm e^\mp \nu\gamma$, $\pi^+\pi^-\pi^0$ and $\pi^0\pi^\pm e^\mp \nu$ backgrounds before setup cuts showing M_ν^2 cut.

Suppressing background due to misreconstructed $z_{K_L^0}$

$z_{K_L^0}$ may be mis-reconstructed for photon candidate pairs that do not originate from a π^0 . Examples are photon pairs from $\pi^0\pi^0$ and $\pi^{\pm}e^{\mp}\nu\gamma$.

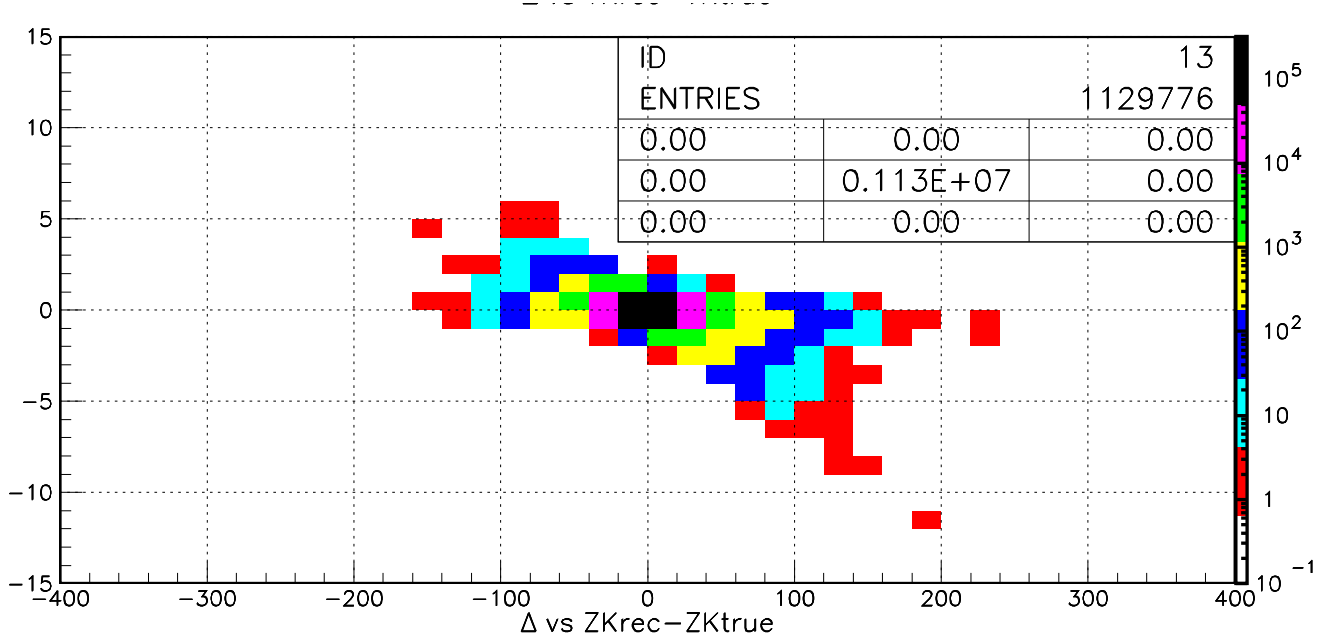

Δ vs $z(K_L^0, \mathrm{recon}) - z(K_L^0, \mathrm{true})$ for $\pi^0\pi^0$ after basic cuts: $|M_{\gamma\gamma} - M(\pi^0)| < 20$ MeV, $\chi^2 < 100$, DOCA < 60 cm, $z_1 < z(K_L^0) < z_2$ cm and the photons are required to pass fiducial cuts to satisfy 2γPR/CAL. DOCA is the distance of closest approach between the measured photon trajectories.

Misreconstructed $z_{K_L^0}$ for 2γPR detection mode

The misreconstruction is caused by large scattering in y direction on 1 γ coupled with energy mismeasurement of one or both γ.

In particular, it occurs when one photon has a relatively small vertical angle. When the γs are not from a π^0 and the energy is mismeasured, imposing the π^0 mass constraint shifts the reconstructed $z_{K_L^0}$.

Note that we preferentially accept $z(K_L^0, \mathbf{recon}) > z(K_L^0, \mathbf{true})$, because $P(K_L^0, \mathbf{recon}) > P(K_L^0, \mathbf{true})$ and $E_{\mathbf{miss}}(\mathbf{recon}) > E_{\mathbf{miss}}(\mathbf{true})$.

There is also correlated effect that makes Δ more negative for $\pi^0\pi^0$: $z(K_L^0, \mathbf{recon}) > z(K_L^0, \mathbf{true})$ sometimes implies $d(\mathbf{recon}) > d(\mathbf{true})$ for $\pi^0\pi^0$ -odd with backward-going photons. ($d \equiv |\vec{x}_{\mathbf{hit}} - \vec{x}_{K_L^0}|$)

Misreconstructed $z_{K_L^0}$ for 2γPR detection mode

Define $\Delta z \equiv z(\mathbf{K_L^0, recon}) - z(\mathbf{K_L^0, true})$

The two useful variables to identify large $|\Delta z|$ are

1. DOCA1+DOCA2 where DOCAi is the distance of closest approach of the $i^{\mathbf{th}}$ measured photon to $z(\mathbf{K_L^0, fit2})$, and
2. $z_1(\mathbf{K_L^0}) - z_2(\mathbf{K_L^0})$ where $z_i(\mathbf{K_L^0})$ is the recon. $z_{\mathbf{K_L^0}}$ from the $i^{\mathbf{th}}$ fit. Fit 1(2) fits the 2 γ to a common vertex without(with) a π^0 mass constraint.

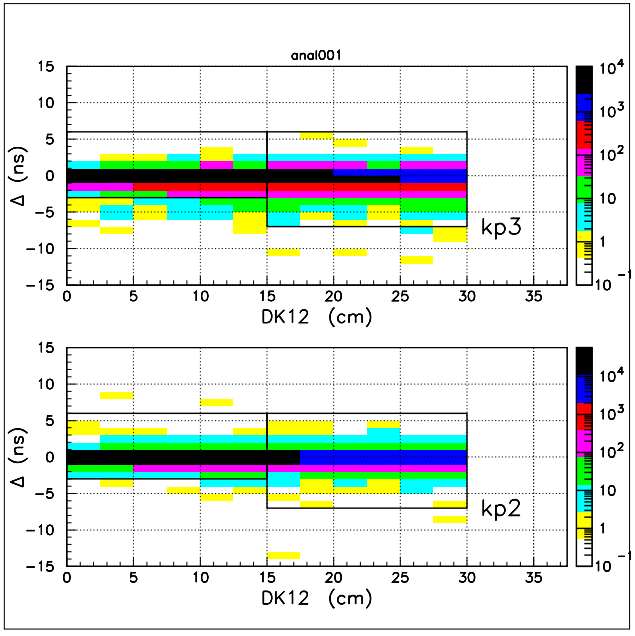

$$\mathbf{DK12} \equiv \sqrt{(\mathbf{DOCA1 + DOCA2 - 5.})^2 + (z_1(\mathbf{K_L^0}) - z_2(\mathbf{K_L^0}))^2}$$

Reject events with $\mathbf{DK12} > \mathbf{30\ cm}$ and use DK12-dependent Δ cut on remainder

Overall results of optimization procedure for all detection methods

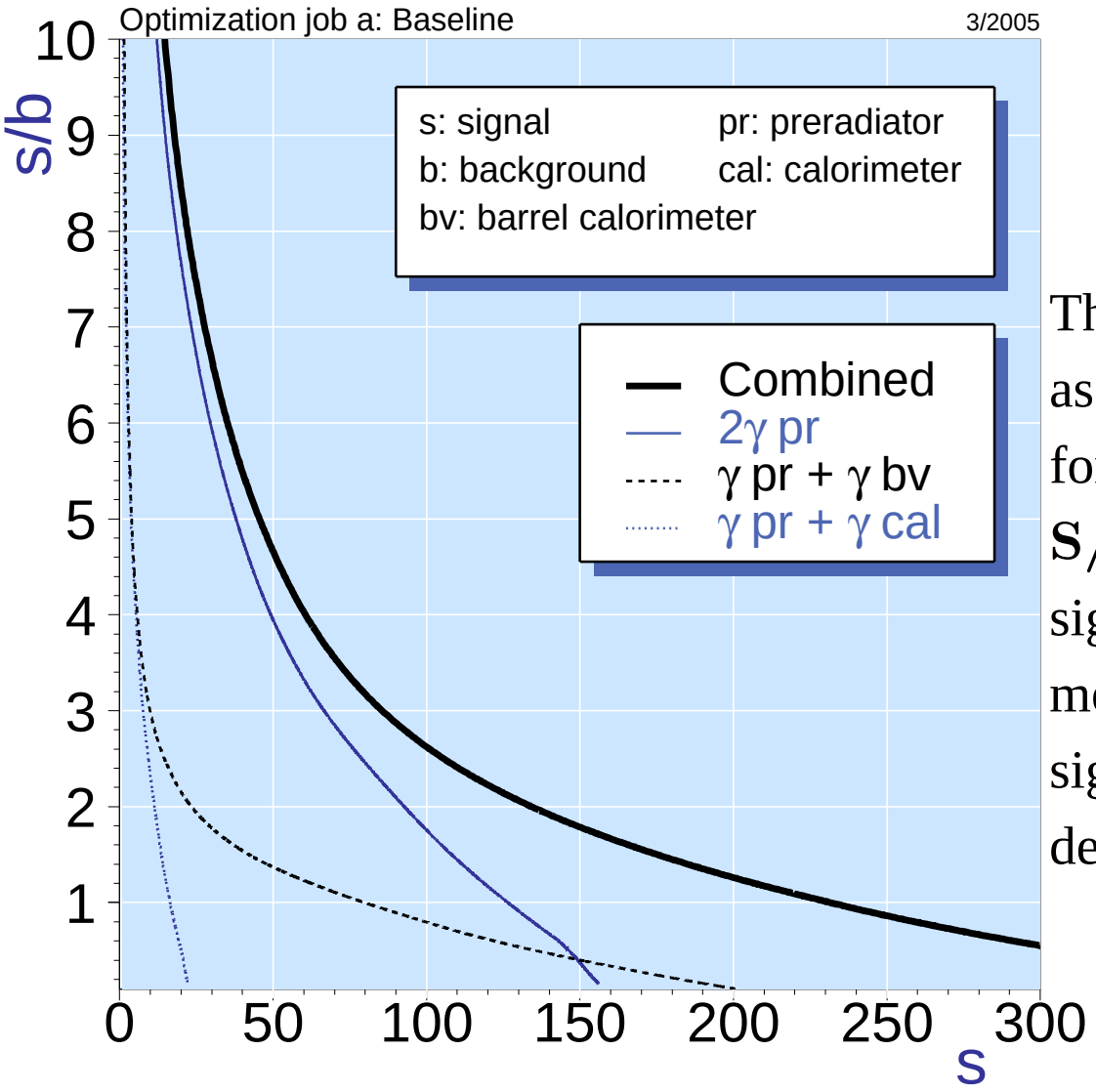

$\mathbf{S/B}$ *vs* $\mathbf{S}$

The signal-to-background rate as a function of the signal yield for all detection methods. At $\mathbf{S/B = 2}$, we expect $\sim \mathbf{130}$ signal events for all detection methods combined and $\sim \mathbf{90}$ signal events for $\mathbf{2\gamma}$PR detection method alone.

Results of optimization procedure, 2γPR, tight cuts

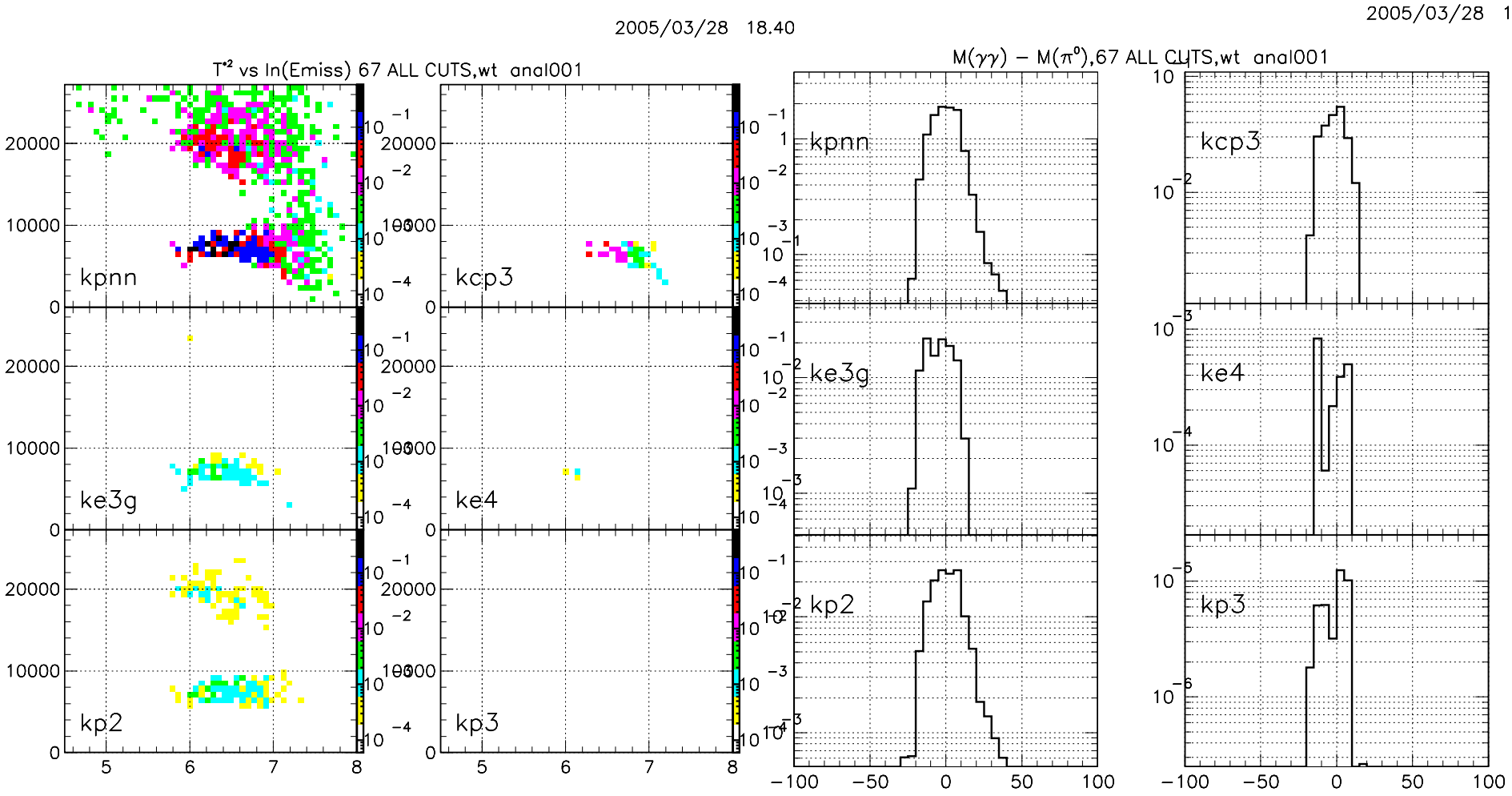

T^{*2} *vs* $\ln(E_{\mathrm{miss}})$

$M(\gamma,\gamma) - M(\pi^0)$

Results of optimization procedure, 2γPR, loose cuts

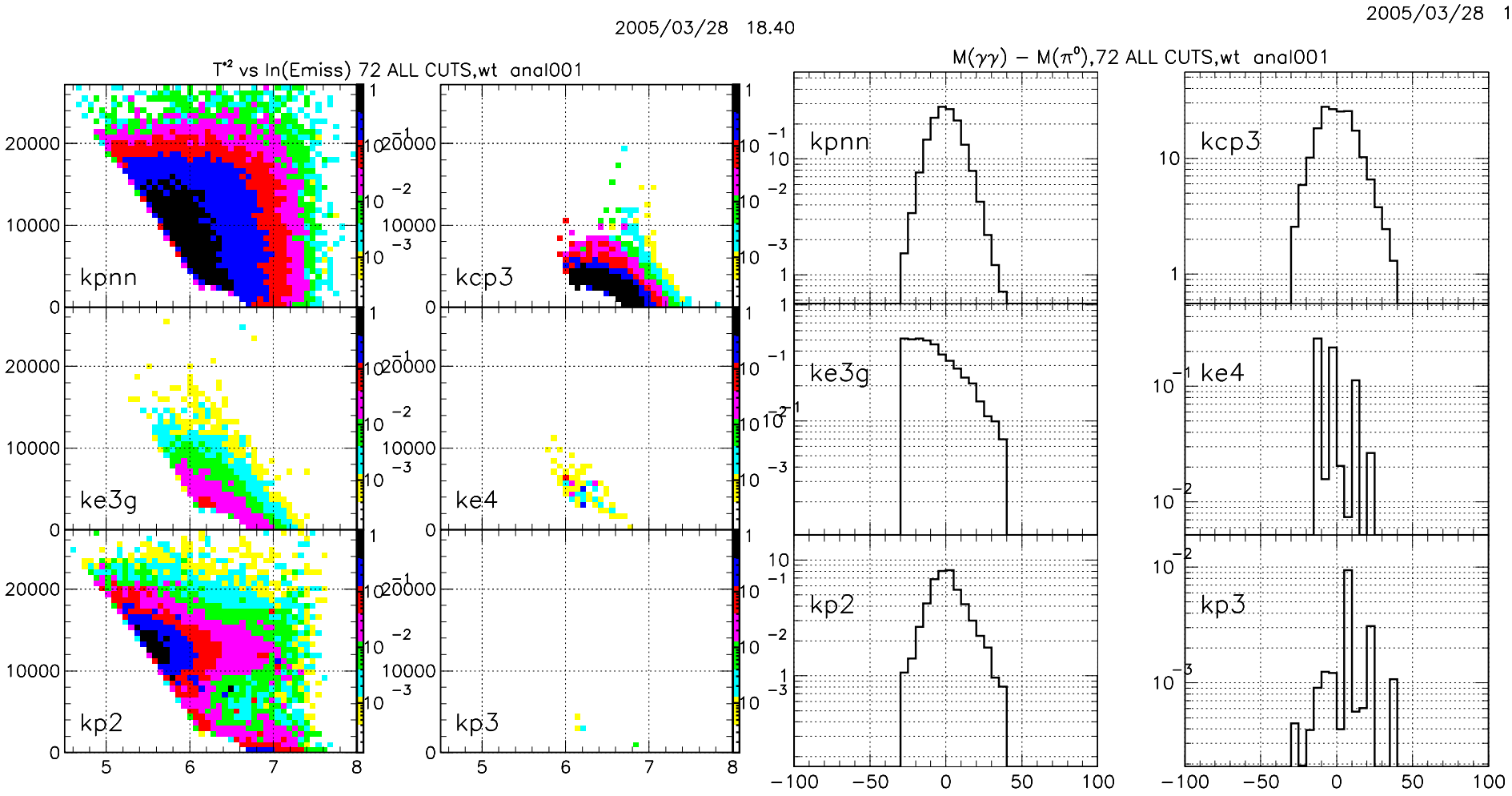

T^{*2} *vs* $\ln(E_{\mathrm{miss}})$

$M(\gamma,\gamma) - M(\pi^0)$

In-bunch backgrounds 2γPR and 1γPR/BV detection modes

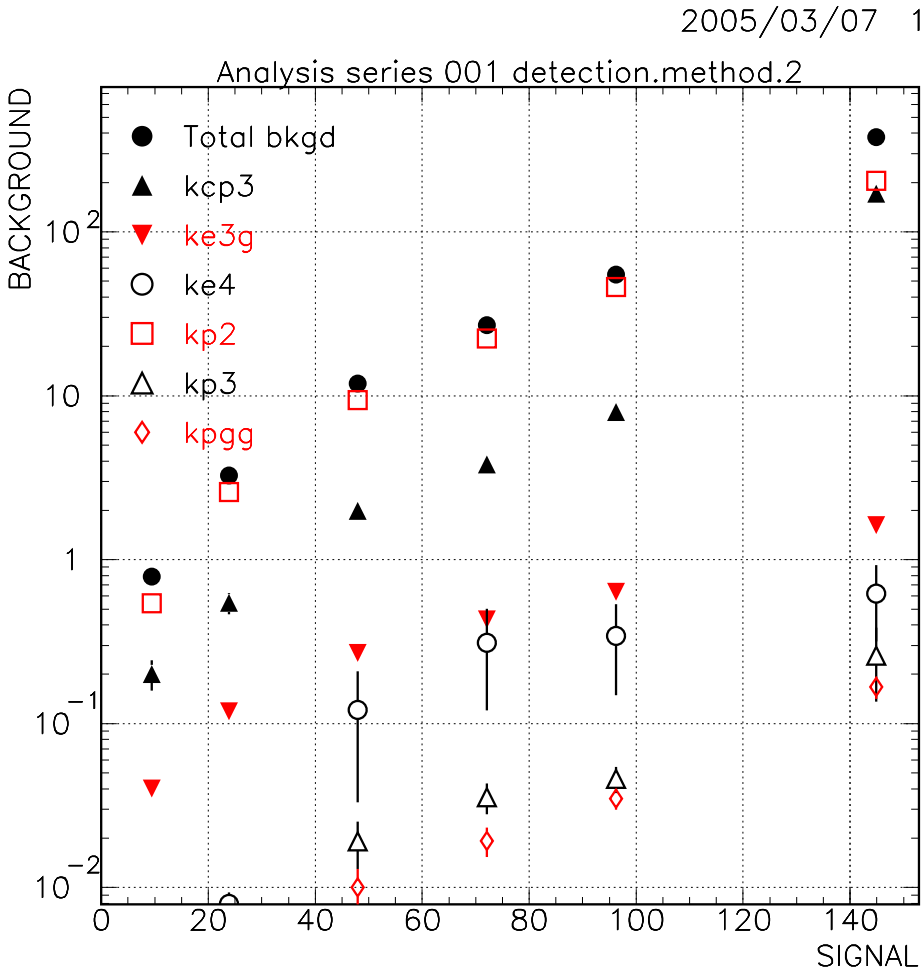

Background *vs* Signal 2γPR

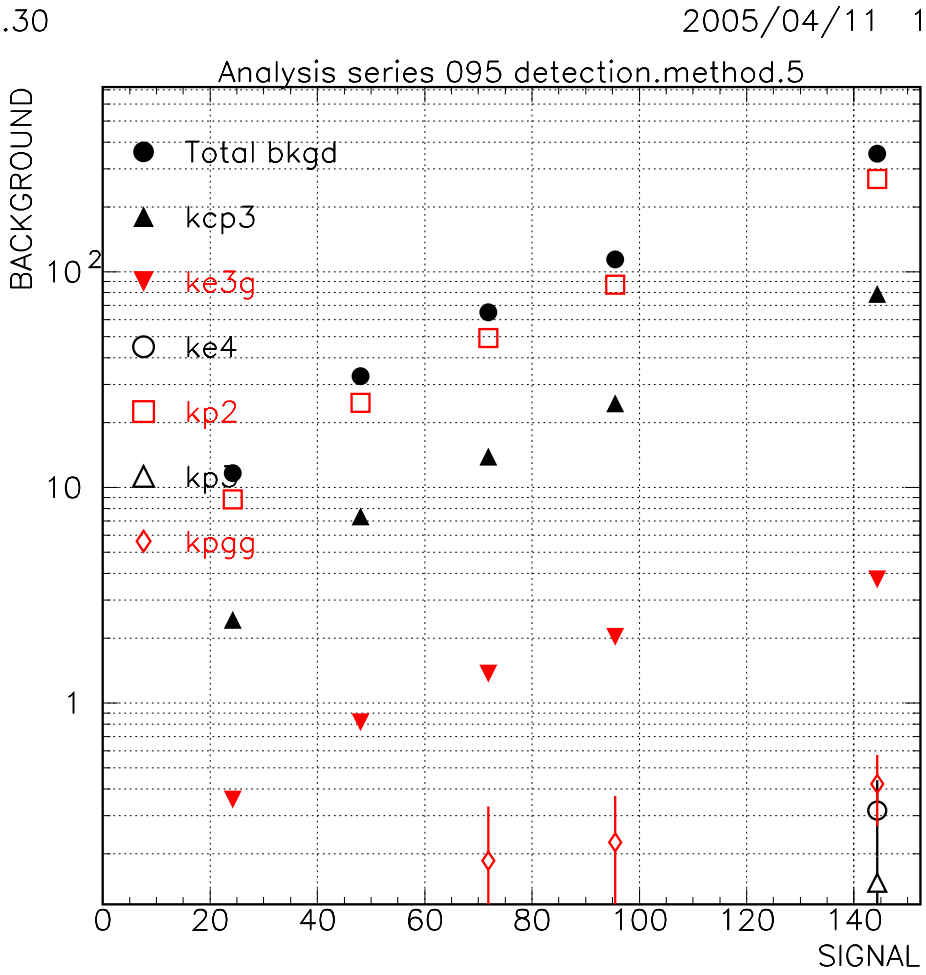

Background *vs* Signal 1γPR/BV

2γPR detection method, interbunch and wrap-around rates

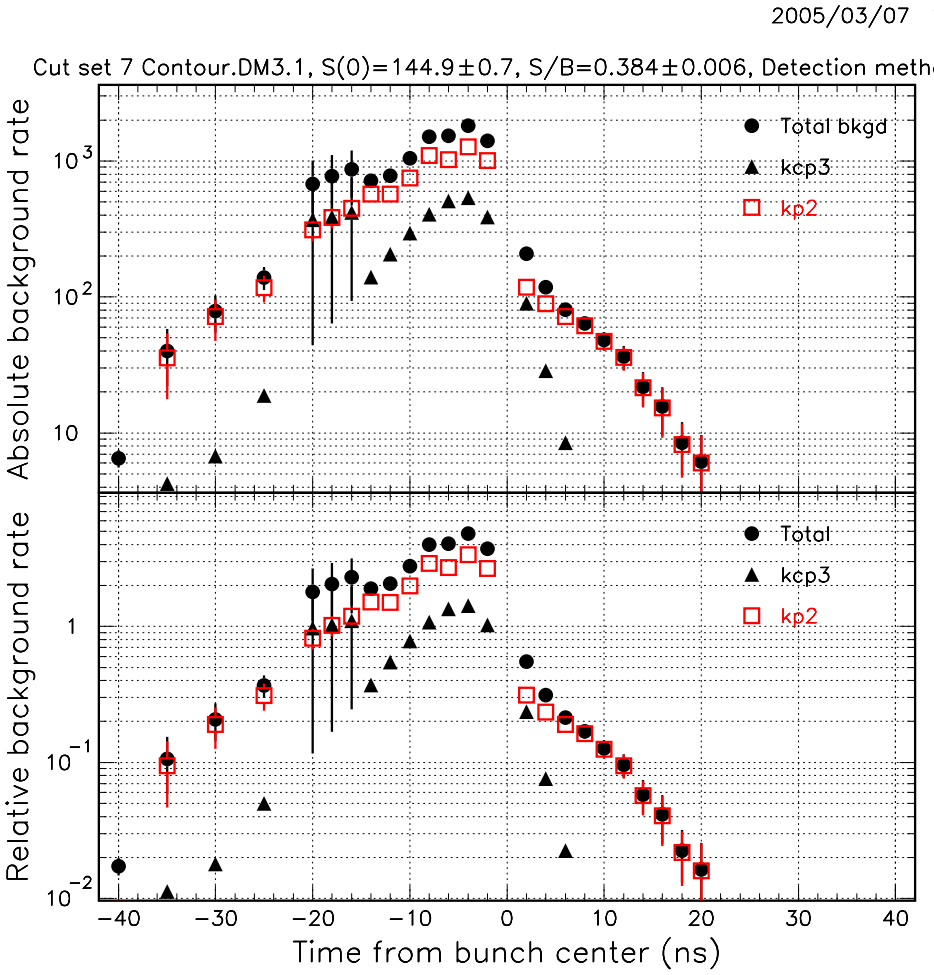

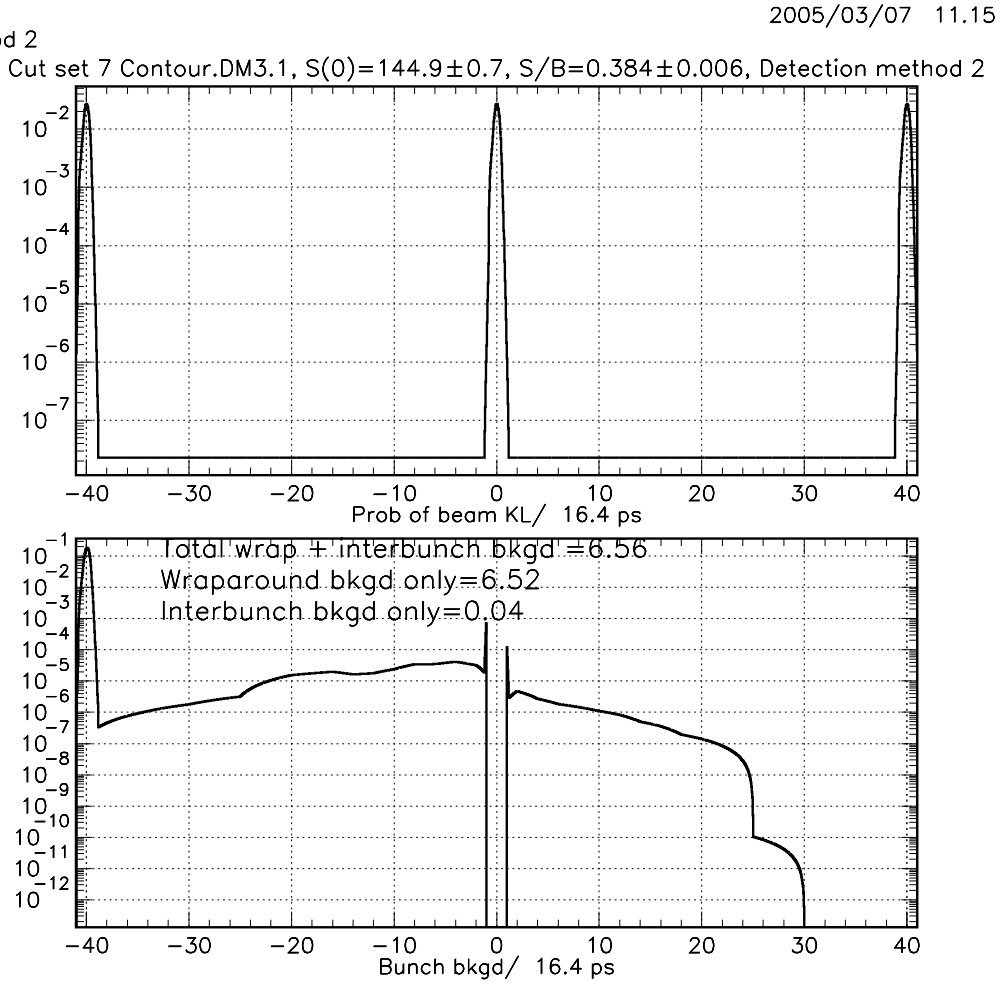

Absolute(top) and relative(bottom) rates *vs* time from bunch center, loosest cuts

Rates given the μbunch prob. dist.

Wrap-around bkgd = 6.52, Interbunch = 0.04

2γPR and 1γPR/BV detection methods, relative wrap-around rates

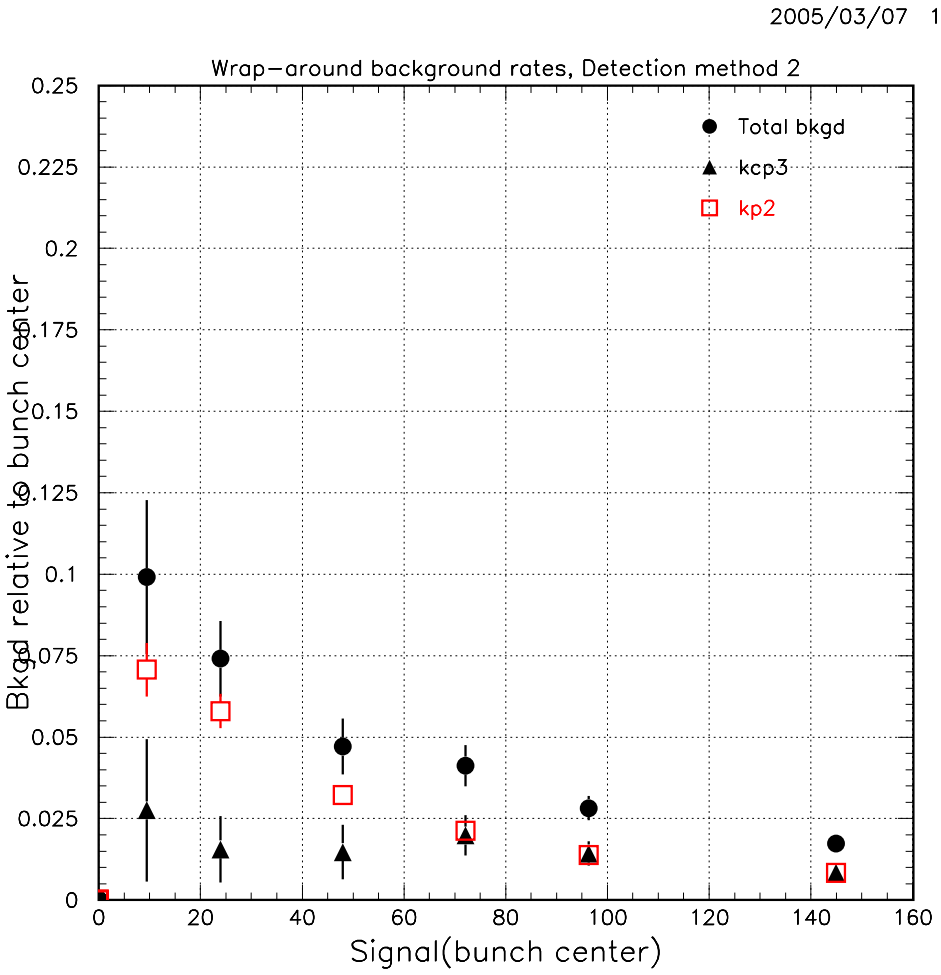

2γPR method

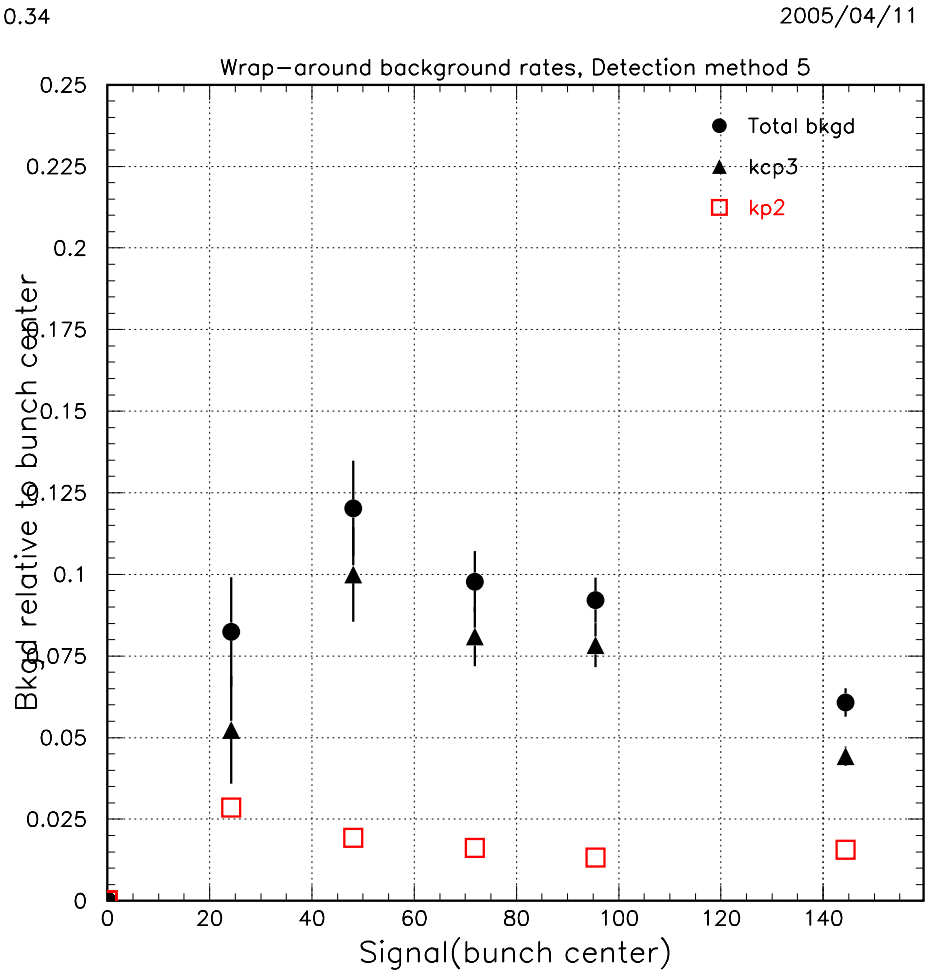

1γPR/BV method

2γPR detection mode, rates with fake & merged γs

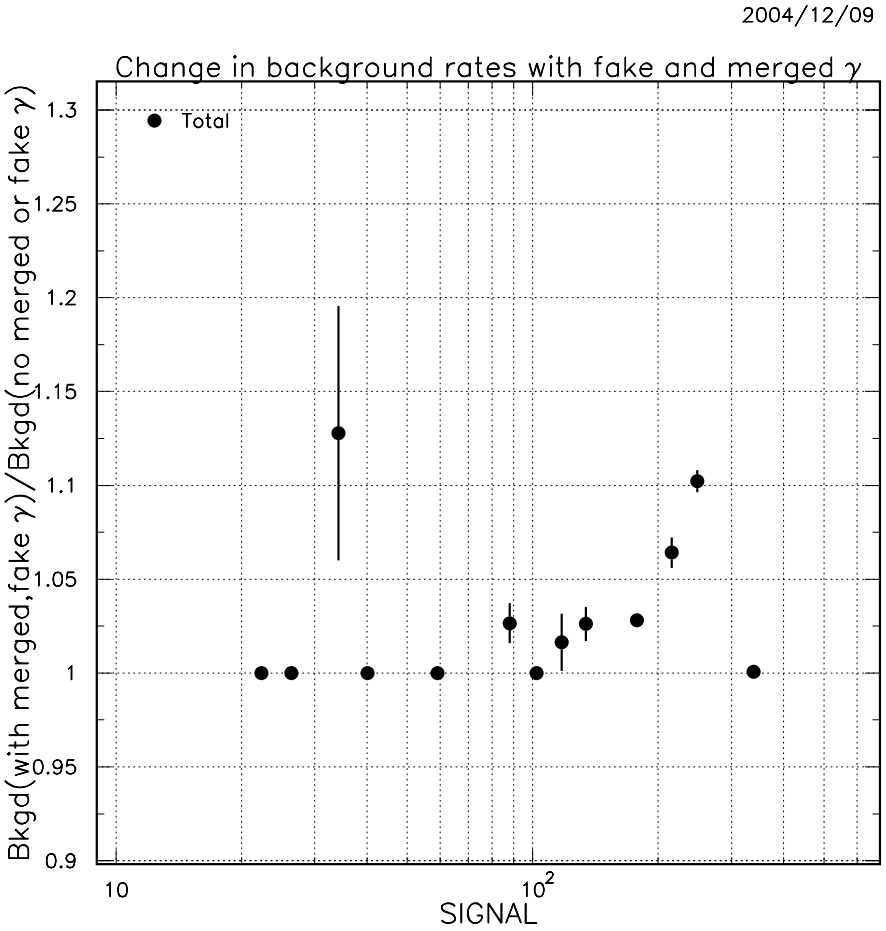

Bkgd(with fake & merged γs)/Bkgd(no fake & merged γs) vs Signal

Fake and merge rates increase background by $\mathbf{1.025 \pm 0.025}$

(Mostly) non-K_L^0 background sources

1. Hyperon background: $< 10^{-5}$ of signal rate
2. $K_S^0 \to \pi^0\pi^0$ background: $\sim 4 \times 10^{-4}$ of $K_L^0 \to \pi^0\pi^0$ background rate
3. $K^{\pm}$ contamination of beam: < 0.001 of signal rate
4. $K_L^0 \to K^{\pm} e^{\mp} \nu$: < 0.001 of signal rate
5. $(K_L^0 \to \pi^{\pm} X) \times (\pi^{\pm} \to \pi^0 e^{\pm} \nu)$: ~ 0.01 of signal rate
6. $nN \to \pi^0 X$: negligible production from residual gas in decay volume if pressure $< 10^{-6}$ Torr. Requirements on reconstructed $z(K_L^0)$ suppress rate from upstream wall to < 0.01 of signal rate.
7. $\bar{n}$: far smaller than neutron background.
8. Fake photons: < 0.05 of signal rate assuming $\sim 10^{-3} \times 10^{-3}$ suppression from (vetoing) $\times$ (γ/n discrimination from shower reconstruction.)
9. Two K_L^0 giving a single candidate: negligible due to veto opportunties

Background from $\Lambda \to \pi^0 n$ ($\mathcal{B}(\Lambda \to n\pi^0) = 35.8\%$)

Due to the soft production spectrum $P(\Lambda) \leq 3.5\ \mathrm{GeV}/c$, Λs that are produced in the target or spoiler are suppressed by $\sim 10^{-17}$ by Λ lifetime ($c\tau = 7.89\ \mathrm{cm}$).

Effect of Λ production at the upstream end of the decay region:

Assume all K_L^0 striking the last 5 cm of a stainless steel beam pipe interact with peak $\sigma(K_L^0 p \to \Lambda\pi^+) = 3.5\ \mathrm{mb}$, K_L^0 halo to the beam is 10^{-4}, 1/10 of the K_L^0 halo interacts in the 5 cm of beam pipe.

If Λ momentum spectrum $\approx$ same as K_L^0 beam, then $\sim 10^{-10}$ of the Λ produced at the upstream end of the decay volume will survive 75 cm to fiducial volume.

$$3.5 \times 10^{-27}\ \mathrm{cm}^2 \times 5\ \mathrm{cm} \times 7.87\ \mathrm{g/cm}^3 \times 6 \times 10^{23} \times 10^{-4} \times 10^{-1} \times 10^{-10} \times 0.358$$
$$\approx 3 \times 10^{-17} << 3 \times 10^{-11}$$

Background from K^0_S Decays ($\mathcal{B}(K^0_S \to \pi^0\pi^0) = 31\%$)

$K^0_S \to \pi^0\pi^0$ decays in the fiducial region would pose the same background problems as $K^0_L \to \pi^0\pi^0$ as sources of in-bunch and interbunch background if the relative rate of K^0_S decays is significant compared to K^0_L decays.

K^0_S lifetime ($c\tau = 2.68$ cm) suppresses K^0_S from target by $\sim 10^{-20}$.

Following Λ background discussion and using $\sigma(K^0_L p \to K^0_S p) = 5.1$ mb, there are $\sim 1.2 \times 10^{-8}$ K^0_S per beam K^0_L so the effective branching fraction relative to the $K^0_L \to \pi^0\pi^0$ rate is

$$\begin{aligned} 1.2 \times 10^{-8} \times \mathcal{B}(K^0_S \to \pi^0\pi^0)/\mathcal{B}(K^0_L \to \pi^0\pi^0) &= \\ 1.2 \times 10^{-8} \times 0.31/(9.32 \times 10^{-4}) &\approx 4 \times 10^{-4} \end{aligned}$$

which is negligible.

Background from Charged Kaons in the Beam

A relative rate of $K^{\pm}/K_L^0 = (2 \pm 1) \times 10^{-7}$ has been determined from GEANT3 simulation of the collimation system and magnets. In addition, the D3 magnet deflects the charged kaons outside the neutral beam envelope which provides an additional suppression of $\sim$1/20 or more (limited by the statistics of the simulation).

Most troublesome $K^{\pm}$ decays have π^0 and single charged track: $\mathcal{B}(K^{\pm} \to \pi^0\pi^{\pm}) = 21.13\%$, $\mathcal{B}(K^{\pm} \to \pi^0\mu^{\pm}\nu) = 3.27\%$, and $\mathcal{B}(K^{\pm} \to \pi^0 e^{\pm}\nu) = 4.87\%$.

The average single charged-track veto inefficiency estimated as $\sqrt{< \bar{\epsilon}_{\pi^+} \times \bar{\epsilon}_{\pi^-} >} = 8.3 \times 10^{-6}$, evaluated for $K_L^0 \to \pi^+\pi^-\pi^0$ decays where $\bar{\epsilon}_{\pi^{\pm}}$ is the veto inefficiency for $\pi^{\pm}$. This estimate is conservative because the majority of the charged kaons are positively charged and $\bar{\epsilon}_{\pi^+} < \bar{\epsilon}_{\pi^-}$. In addition, $\bar{\epsilon}(\mathrm{lepton}) < \bar{\epsilon}_{\pi^+}$.

So the upper limit on the relative rate from charged kaon decays is

$$2 \times 10^{-7} \times 0.05 \times 0.29 \times 8.3 \times 10^{-6}/3 \times 10^{-11} \approx 8 \times 10^{-4} \ .$$

Background from $K_L^0 \to K^\pm e^\mp \nu$

Background from K_L^0 beta decay is similar to background from charged kaons in the beam.The expected rate relative to the signal is

$$\mathcal{B}(K_L^0 \to K^\pm e^\mp \nu) \times \mathcal{B}(K^\pm \to \pi^0 X) \times \bar{\epsilon}_X / \mathcal{B}(K_L^0 \to \pi^0 \nu\bar{\nu}) \approx$$
$$1. \times 10^{-8} \times 0.29 \times 8.3 \times 10^{-6} / 3 \times 10^{-11} = 8 \times 10^{-4}$$

where $K^\pm \to \pi^0 X$ is the sum of the three charged kaon decays to a π^0 and single charged track: $\mathcal{B}(K^\pm \to \pi^0 \pi^\pm) = 21.13\%$, $\mathcal{B}(K^\pm \to \pi^0 \mu^\pm \nu) = 3.27\%$, and $\mathcal{B}(K^\pm \to \pi^0 e^\pm \nu) = 4.87\%$, with a total branching fraction of 29%, $\bar{\epsilon}_X$ is the estimated veto inefficiency for the charged track, and the SM values of $K_L^0 \to K^\pm e^\mp \nu$ and signal are used.

Background from $\pi^{\pm} \to \pi^0 e^{\pm} \nu$

Charged pion beta decay ($\mathcal{B}(\pi^{\pm} \to \pi^0 e^{\pm} \nu) = 1.025 \times 10^{-8}$) is a potential source of background when the charged pion is the result of K_L^0 decay. Since $P(\pi^0) \approx P(\pi^{\pm})$, the decay chain $K_L^0 \to \pi^{\pm} e^{\mp} \nu$, $\pi^{\pm} \to \pi^0 e^{\pm} \nu$ (Ke3) is the most dangerous of this type of background because the dynamics and kinematics of the pion from K_L^0 decay are very similar to that of the π^0 from $K_L^0 \to \pi^0 \nu \bar{\nu}$. The other three-body semileptonic decay $K_L^0 \to \pi^{\pm} \mu^{\mp} \nu$ (Km3) is less dangerous because the kinematics differs from that of the signal.

The relative rate of the Ke3 (Km3) with pion beta decay to the SM signal rate is 129.4 (90.6).

Background from $\pi^{\pm} \to \pi^{0} e^{\pm} \nu$ (continued)

The two semileptonic decays were studied with the FastMC. "Fiducial cuts" requiring the reconstructed π^0 vertex to lie within the beam envelope suppresses Ke3 (Km3) by $\mathbf{160}$ $(\mathbf{140})$ with no significant loss of signal acceptance. Requiring $\Delta > -5$ ns for the lepton from the K_L^0 suppresses Ke3 (Km3) by $\mathbf{8.5}$ $(\mathbf{39.5})$. The effect of this cut is to select pion beta decays significantly displaced from the K_L^0 decay vertex. It is more effective on Km3 because the pion has lower momentum and the $\beta < 1$ muon compensates for the displacement between the K_L^0 and pion decay vertices. Additional suppression is possible by detecting the $e^{\pm}$ (e_π) from pion beta decay. The fiducial cuts select a harder e_π spectrum because the $\pi^{\pm}$ is required to be more forward in the lab. Conservatively assuming that e_π above 2 MeV can be vetoed suppresses Ke3 (Km3) by $\mathbf{9.2}$ $(\mathbf{9.1})$.

Assuming the contribution of $K_L^0 \to \pi^+\pi^-\pi^0$ is negligible due to the reduced phase space and veto opportunities, the contribution of $K_L^0 \to \pi^{\pm}\ell^{\mp}\nu$, $\pi^{\pm} \to \pi^0 e^{\pm}\nu$ is $\sim \mathbf{0.012}$ of the signal rate. (More details on next page).

Background from $\pi^{\pm} \to \pi^0 e^{\pm} \nu$ (continued)

FastMC estimate of $K_L^0 \to \pi^{\pm}\ell^{\mp}\nu$, $\pi^{\pm} \to \pi^0 e^{\pm}\nu$ background. In the table $\mathcal{B}(K) = \mathcal{B}(K_L^0 \to \pi^{\pm}\ell^{\mp}\nu)$, $\mathcal{B}(\pi) = \mathcal{B}(\pi^{\pm} \to \pi^0 e^{\pm}\nu)$, and $\mathcal{B}(\mathrm{s}) = \mathcal{B}(K_L^0 \to \pi^0\nu\bar{\nu})$. The upper portion of the table gives the number of surviving candidates after the listed cuts. The lower portion of the table has the background rate relative to the signal after successive cuts.

Cut	$K_L^0 \to \pi^{\pm}e^{\mp}\nu$	$K_L^0 \to \pi^{\pm}\mu^{\mp}\nu$	
None	300000	200000	
Fiducial	1871	1445	
$E(e_\pi) < 2$ MeV	204	158	
$\Delta > -5$ ns	24	4	
$\mathcal{B}(K)$	0.3881	0.2719	
	Rate relative to signal		
$\mathcal{B}(K)\mathcal{B}(\pi)/\mathcal{B}(\mathrm{s})$	129.4	90.6	
$\times\epsilon(\mathrm{Fiducial})$	0.802	0.652	
$\times\epsilon(\Delta) \times \epsilon(e_\pi)$	$\mathbf{0.010 \pm 0.002}$	$\mathbf{0.002 \pm 0.001}$	

$nN \to \pi^0 X$ background

Two potential sources of $nN \to \pi^0 X$ background ($X =$ invisible):

1. Interactions of n beam with residual gas in decay region and
2. interactions of n halo with beam pipe or detector at upstream (US) and downstream (DS) ends of the decay region.

FastMC was used to produce $nN \to \pi^0 X$ according to phase space and baryon number conservation. Assume entire nN cross-section (35 mb) above π^0 production threshold is due to $nN \to \pi^0 X$. Neutron beam momentum spectrum taken from measurements at $46.5°$. Assume n halo momentum spectrum to be the same as n beam, $(n\ \mathbf{halo})/(n\ \mathbf{beam}) = 10^{-4}$, $(n\ \mathbf{beam})/(\mathrm{K_L^0}\ \mathbf{beam}) = 1000$. Residual gas in decay region approximated by air at 10^{-7} Torr.

With these assumptions, total rate of n background from interactions in residual gas $< 1\%$ after loose kinematic cuts.

$nN \rightarrow \pi^0 X$ background (continued)

Neutron interactions were generated at the US and DS ends of the decay volume. The US (DS) active region was assumed to be 0.56 cm of Pb (15 cm of polysterene). The possibility that neutron interactions generated additional particles that could serve to veto the event was ignored.

Fiducial cuts on $z(K)$, the reconstructed z of the $\mathbf{K_L^0}$ candidate vertex suppress the relative n background to signal rate to be $\sim \mathbf{1\%}$. For the $\mathbf{2}\gamma$PR ($\mathbf{1}\gamma$PR) detection methods, $z(K)$ is required to be 75 cm (100 cm) and 50 cm (100 cm) from the US and DS ends of the decay region, respectively.

Additional suppression with slight acceptance would be possible with cuts on the χ^2 and/or the reconstructed π^0 time and momentum (figures next page).

$nN \rightarrow \pi^0 X$ background (continued)

2002/12/23 12.07

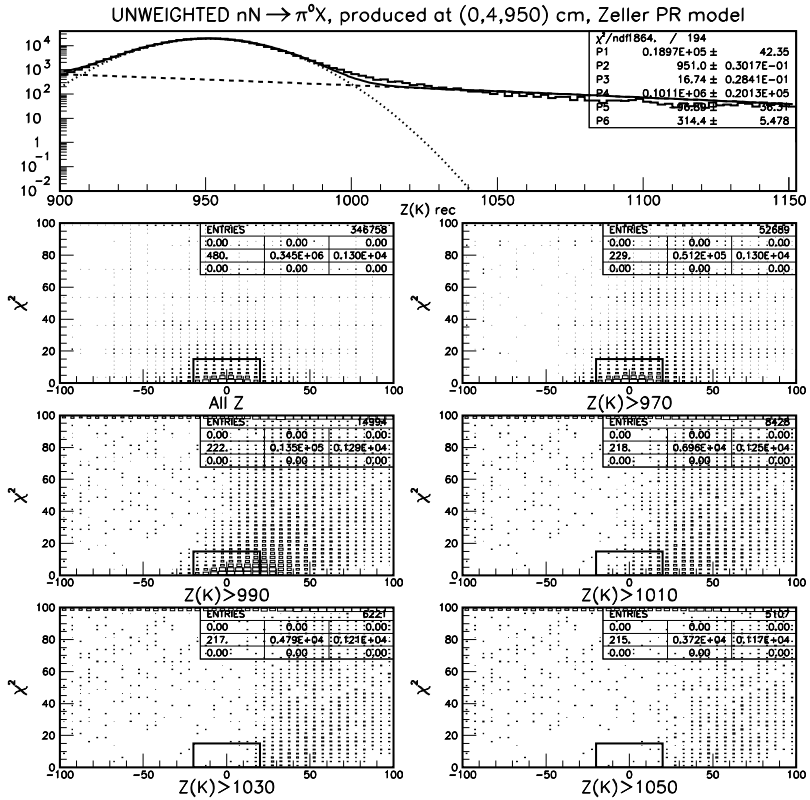

Top:The reconstructed $z(K)$ distribution for $nN \rightarrow \pi^0 X$ production at (0,4,950) cm fitted with a double Gaussian. (For this study, the decay region extended from 950 to 1350 cm.) Other: χ^2 *vs.* $M_{\gamma\gamma} - M_{\pi^0}$ in MeV for increasingly harder cuts on $z(K)$. The box in these plots corresponds to $\chi^2 < 15$ and $|M_{\gamma\gamma} - M_{\pi^0}| < 20$ Mev.

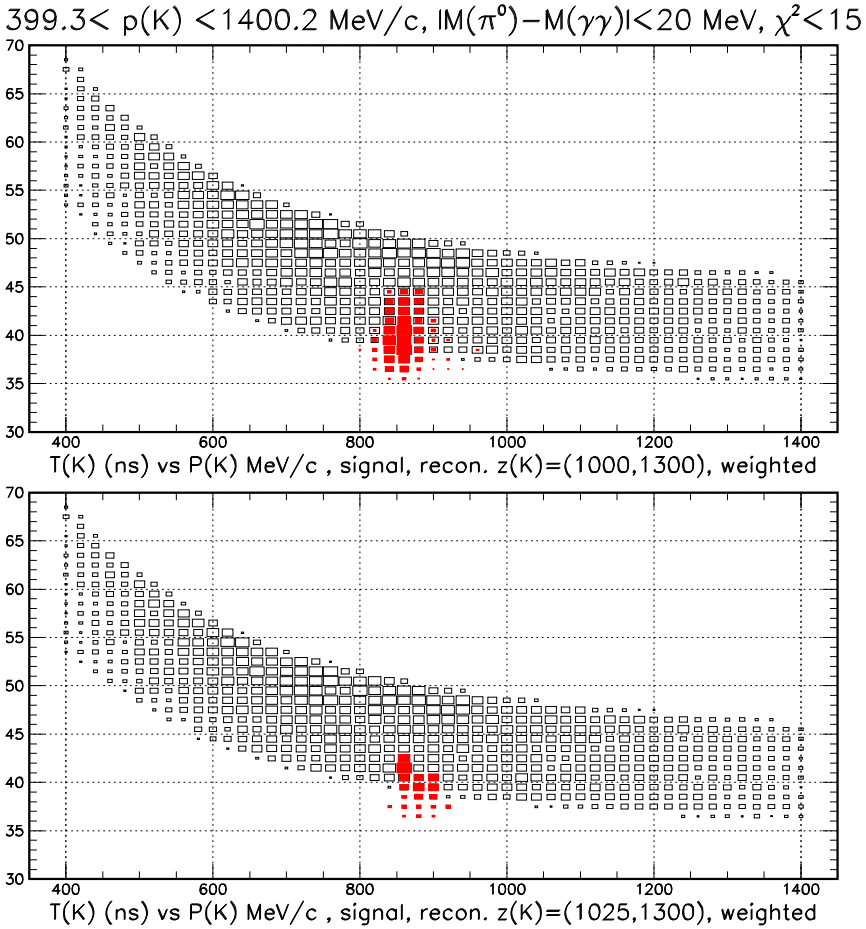

Comparison of the reconstructed kaon decay time *vs.* reconstructed kaon momentum for signal(black) and neutron halo(red) events.

$\bar{n}$ background

From GEANT3 simulation, the rate of $\bar{n}$ production from the KOPIO target is $\mathbf{3.9 \times 10^{-3}}$ times the rate for n production for neutron momentum above $\mathbf{775\ MeV/c}$ (approximate π^0 production threshold).

The relative production rate of π^0 for $\bar{n}$ and $n(p > 775\ \mathrm{MeV}/c)$ in the residual gas was determined to $\sim \mathbf{2.5}$.

Rate of potential π^0 candidates from $\bar{n}$ interactions to that of n interactions is $(\mathbf{3.9 \times 10^{-3}}) \times \mathbf{2.5} \approx \mathbf{0.01}$.

Uncertainties in overall expected acceptance

Based on measurements and calculations we assess these relative ranges on the following parameters.

Range	Parameter
$\mathbf{1.0 \pm 0.2}$	$\mathbf{K_L^0}$ flux
$\mathbf{1.0 \pm 0.11}$	Survival factor due to other $\mathbf{K_L^0}$ in microbunch
$\mathbf{1.0 \pm 0.25}$	Effect of photon veto on acceptance
$\mathbf{1.0^{+0.3}_{-0.2}}$	Effect of charged particle veto on acceptance
$\mathbf{1.0 \pm 0.2}$	Veto gate scale factor
$\mathbf{1.0 \pm 0.5}$	Neutron beam core
$\mathbf{1.0^{+1.0}_{-0.5}}$	Neutron halo/beam
$\mathbf{1.0^{+1.0}_{-0.4}}$	Neutron response factor

The ranges are taken into account into evaluating the expected precision on $\mathcal{B}(\mathrm{K_L^0} \to \pi^0 \nu\bar{\nu})$.

Spill length optimization taking uncertainties into account

2005/04/15 15.28

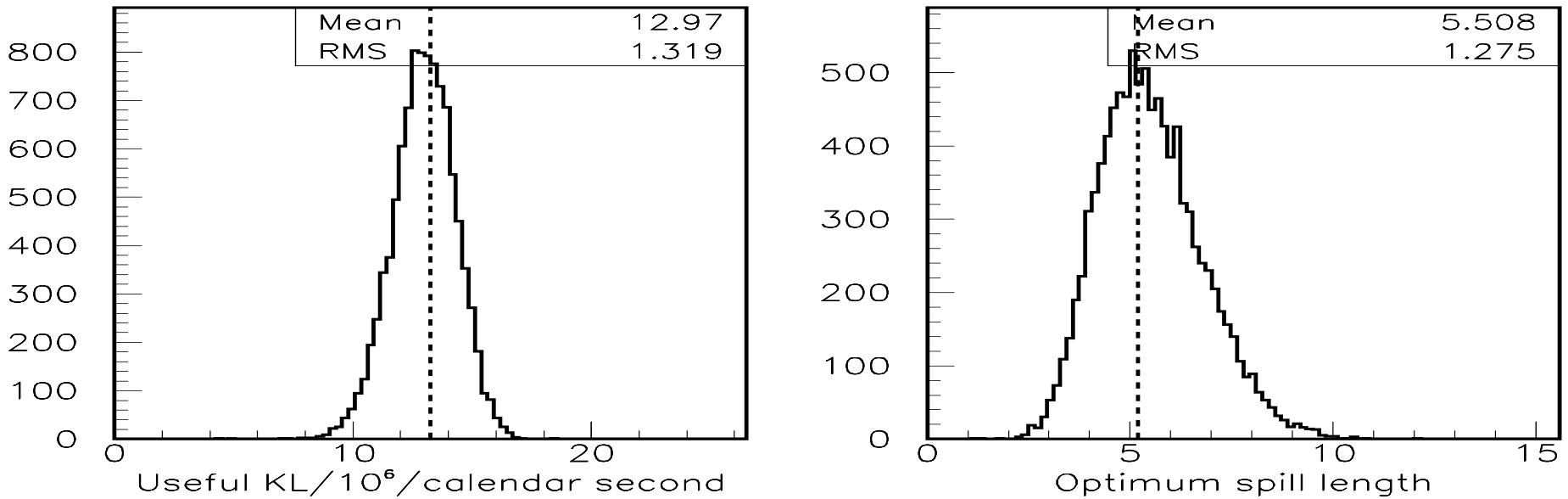

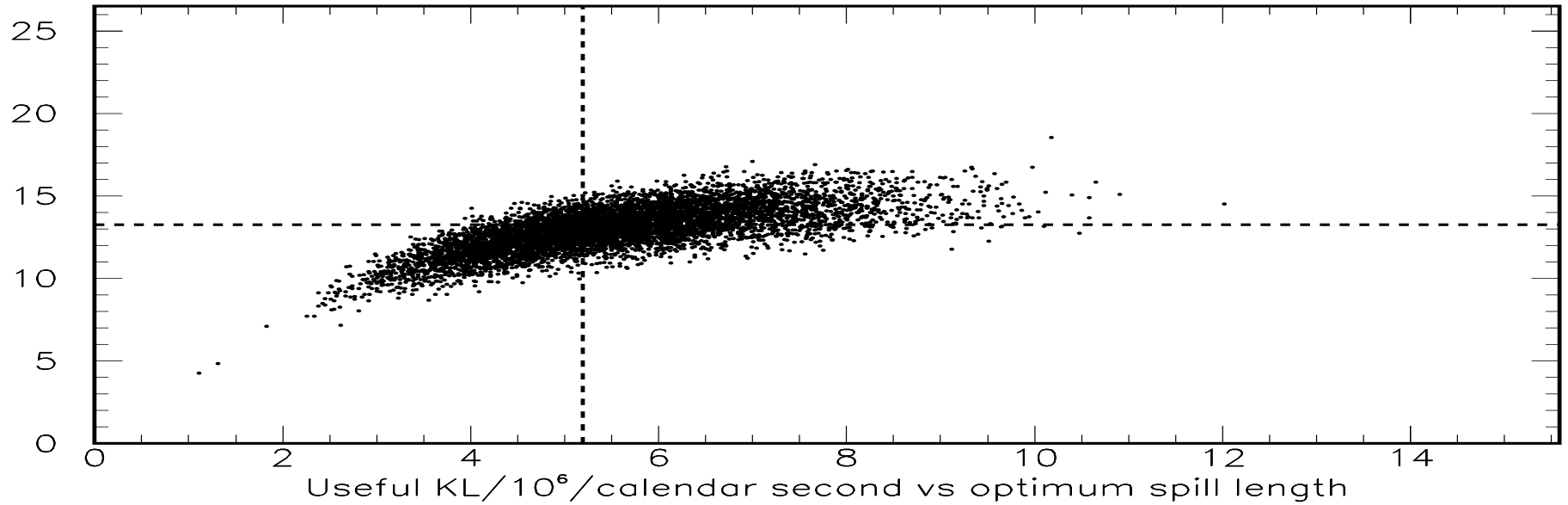

$\mathcal{B}(K_L^0 \to \pi^0 \nu\bar{\nu})$ precision and sensitivity

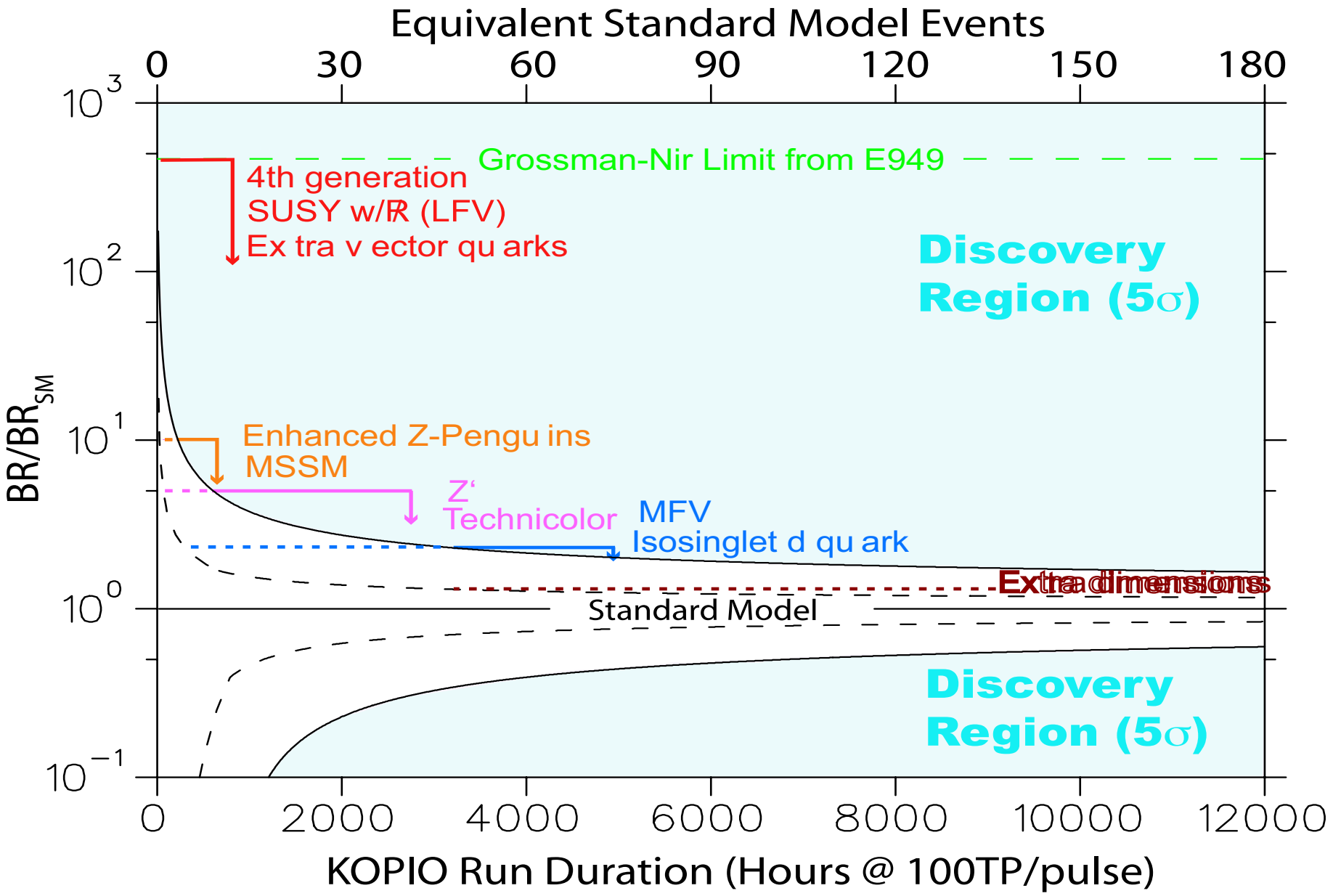

Extras

Some outstanding issues

1. More robust estimates of losses from trigger and reconstruction with GEANT (in progress)
2. Continued study of E949 to understand issues of PV inefficiency and comparison with FLUKA and GEANT4 simulations
3. More robust estimate of rejection of “fake photons” in PR from GEANT

$\gamma\gamma$ opening angle at PR in degrees

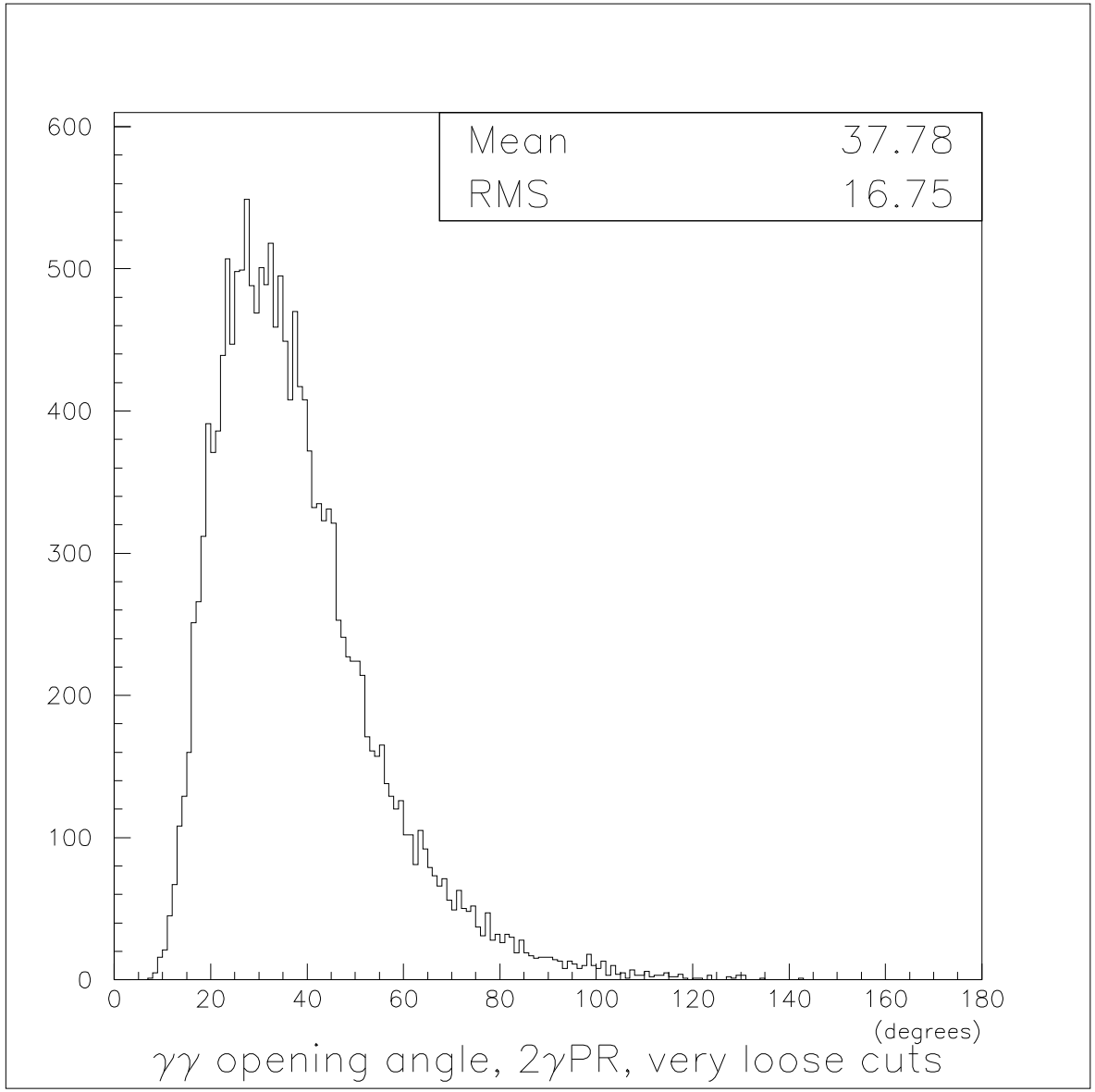

Signal loss due to removal of 1 PR module

PR thickness in radiation lengths $= \mathbf{2.7}$

$\mathbf{Yield} \propto (1 - e^{-\frac{7}{9}\mathbf{2.7}})^{\mathbf{2}} = \mathbf{0.8775^2} = \mathbf{0.770}$

Loss of one module would reduce PR thickness to $\frac{\mathbf{7}}{\mathbf{8}}\mathbf{2.7} = \mathbf{2.36}$ rad. len.

$\mathbf{Yield} \propto (1 - e^{-\frac{7}{9}\frac{7}{8}\mathbf{2.7}})^{\mathbf{2}} = \mathbf{0.8047^2} = \mathbf{0.648}$

$\mathbf{Ratio} = \mathbf{0.648/0.770} = \mathbf{0.841}$

Removal of 1 PR module entails a signal loss of $\sim \mathbf{16\%}$.

Dead material and gaps between PV modules

We performed a GEANT3 study of the effect of dead material and air gaps between the modules of the barrel photon veto. For the purpose of the study, each PV module was encased in a 'wrapper' composed of either iron or air. $K_L^0 \rightarrow \pi^0\pi^0$ decays were generated in the decay volume and at least two photons were required to strike the PR. The PV inefficiency of the remaining photons was investigated.

Conclusions drawn from figures on next pages:

1. There is essentially no change in the photon veto inefficiency for up to 2 mm of dead material (iron) between barrel veto modules for a 1 MeV threshold.
2. There is no change in the photon veto inefficiency for up to 4 mm of air between barrel veto modules for thresholds up to 5 MeV.

Based on additional simulation, we expect similar behavior for other photon vetos including the calorimeter. We expect ≤ 0.5 mm of material between modules for the photon vetos and the calorimeter. The cables and support for these detectors are external to the active elements; support for the CPV is small and the cables egress non-projectively. The PV performance is based on measurements on a real detector with cracks, cables, etc.

Dead material between PV modules (GEANT3 study)

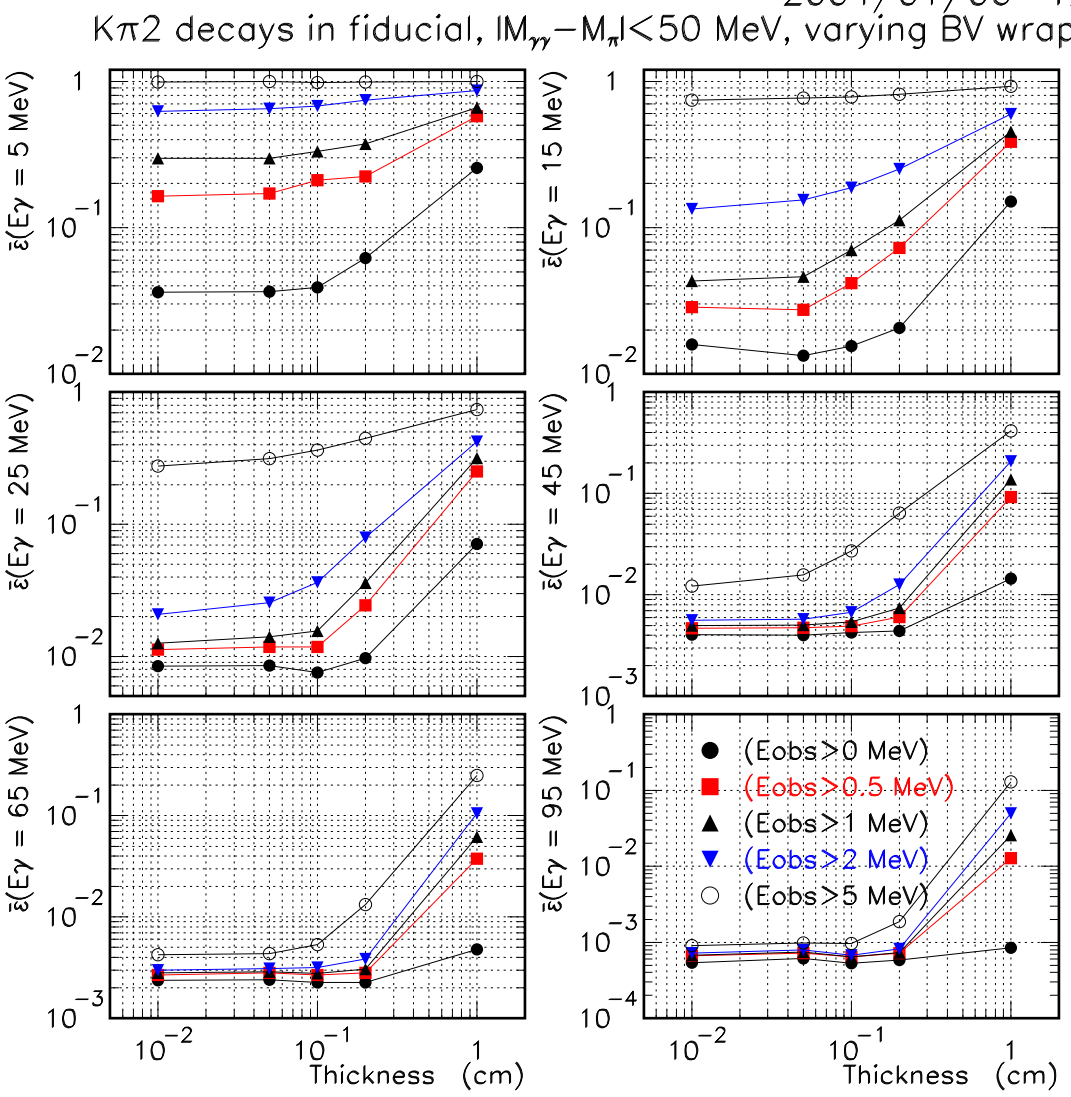

Photon veto inefficiency as a function of iron wrapper thickness and energy threshold for six photon energies. (E_{obs} is approximately a third of the deposited energy.) The photon energy range is ± 5 MeV about the value given, so the upper right plot is for $10 < E_\gamma < 20$ MeV. There is essentially no change in the photon veto inefficiency for up to 2 mm of dead material (iron) between barrel veto modules for a 1 MeV threshold.

Air gaps between PV modules (GEANT3 study)

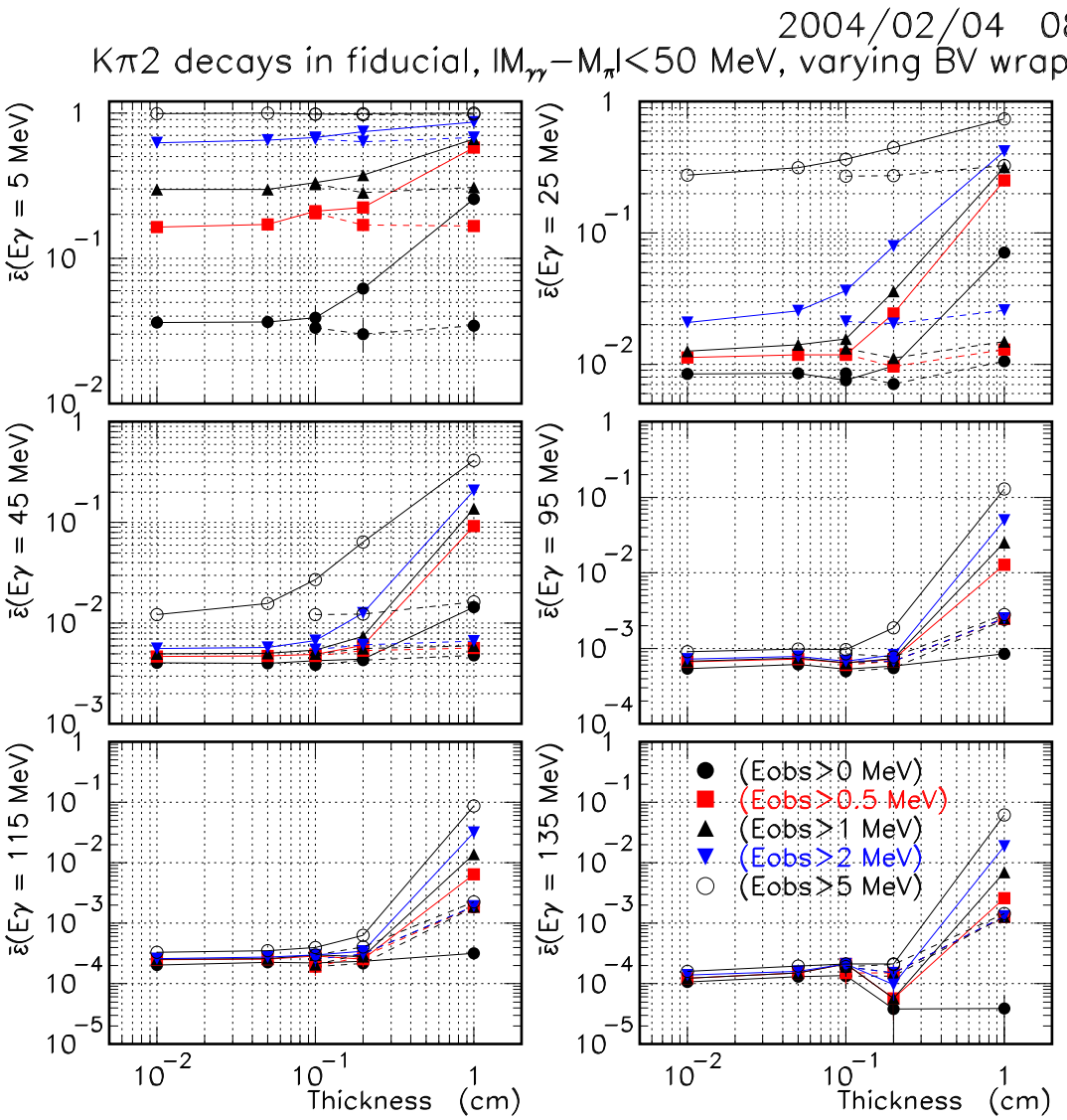

Photon veto inefficiency as a function of wrapper thickness and energy threshold for six photon energies.

Points with the same energy threshold connected with a **solid line** correspond to an **iron wrapper**. Points connected with a **dashed line** correspond to an **air wrapper**.

There is no change in the photon veto inefficiency for up to 4 mm of air between barrel veto modules for thresholds up to 5 MeV.

100 MHz Cavity

We have measured a microbunch width of 242 ps for a 93 MHz cavity at 22 kV. Our simulation predicts a width of 217 ps for the same configuration. Since the 93 MHz cavity is very similar to the 100 MHz KOPIO cavity, the good agreement in microbunch widths gives us confidence that the 100 MHz cavity will be able to produce the required time structure.

However there is a factor of 2 discrepancy between the simulated and measured widths at 4.5 MHz that is not yet fully understood. The measured microbunch width of 1950 ps for 4.5 MHz at 270 kV can be compared with the simulated width of 930 ps.

We have simulated the behavior of the KOPIO configuration (25 MHz and 100 MHz both at 150 kV) and predict a width of 180 ps. The 25 MHz cavity alone would give a width of 238 ps according to our simulation.

We have confidence in the predictive power of the simulation for the two-cavity KOPIO configuration because the widths at 93 MHz agree at the 10% level. But our confidence in the predicted width for the 25 MHz cavity alone is not high enough to obviate the need for the 100 MHz cavity.

Microbunch width studies

We performed FastMC studies of the effect of increasing the microbunch width from the nominal value of 200 ps.

Conclusions drawn from figures on the next pages:

- Approximately 17% of the events at the highest signal-to-background are lost if the microbunch width is increased to 300 ps.
- We need an accurate measure of the microbunch width to achieve optimal sensitivity.

Events at the highest signal-to-background are essential in establishing the existence of the $\mathbf{K_L^0 \rightarrow \pi^0 \nu \bar{\nu}}$ decay.

Test beam measurements show we can accurately measure the microbunch width with a $\mathbf{90^\circ}$ monitor observing the neutral beam production target if it does not vary too quickly. The possible extent and timescales of the variation is not completely known.

In addition, as the microbunch width becomes large with respect to the intrinsic time resolution of the detector, the degree of precision that's needed to obtain the optimal sensitivity becomes greater.

Microbunch width studies

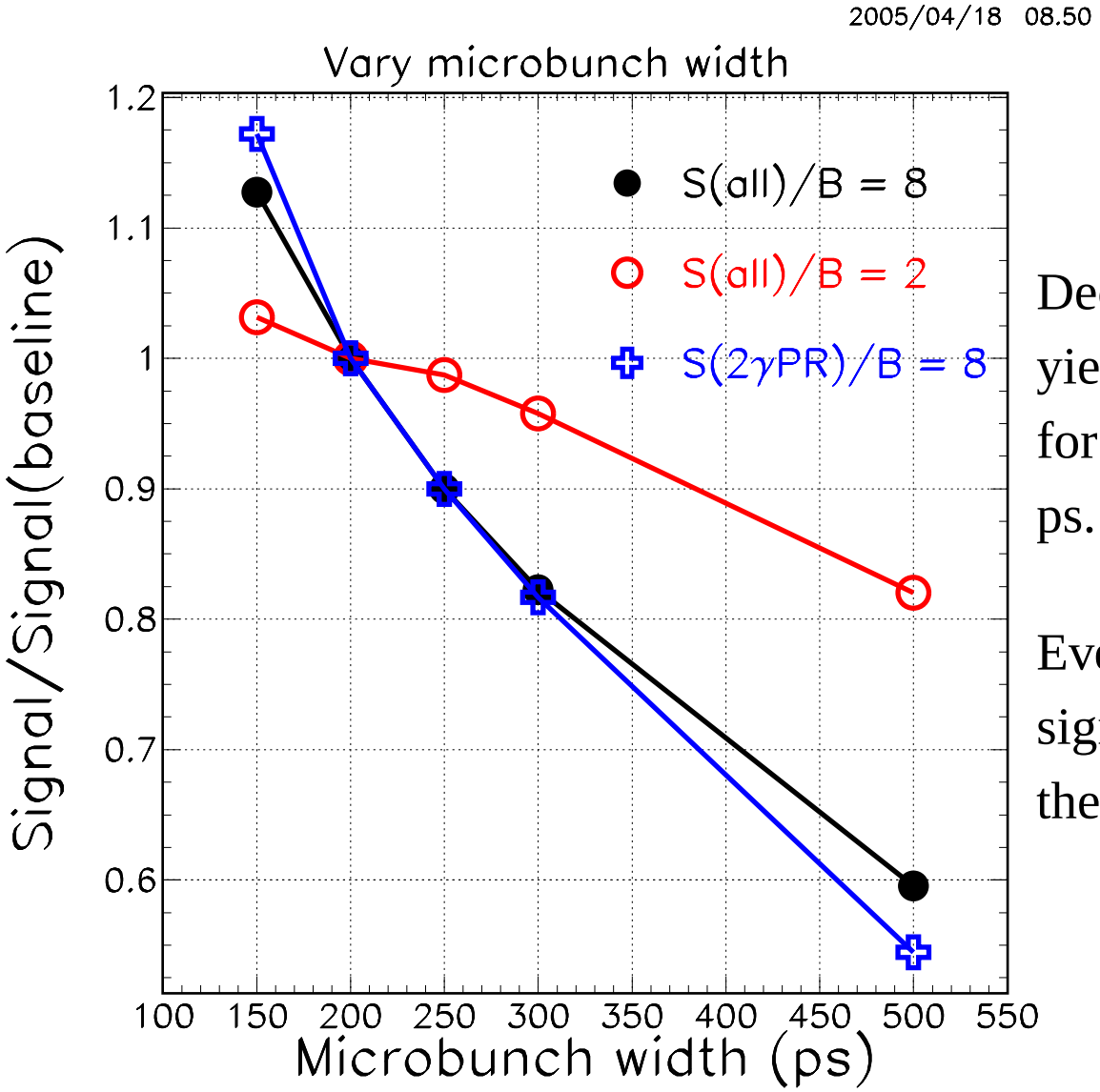

Decrease in optimized signal yield as the microbunch width for a range from 150 ps to 500 ps.

Events with the highest signal-to-background are lost as the width increases.

Microbunch width studies

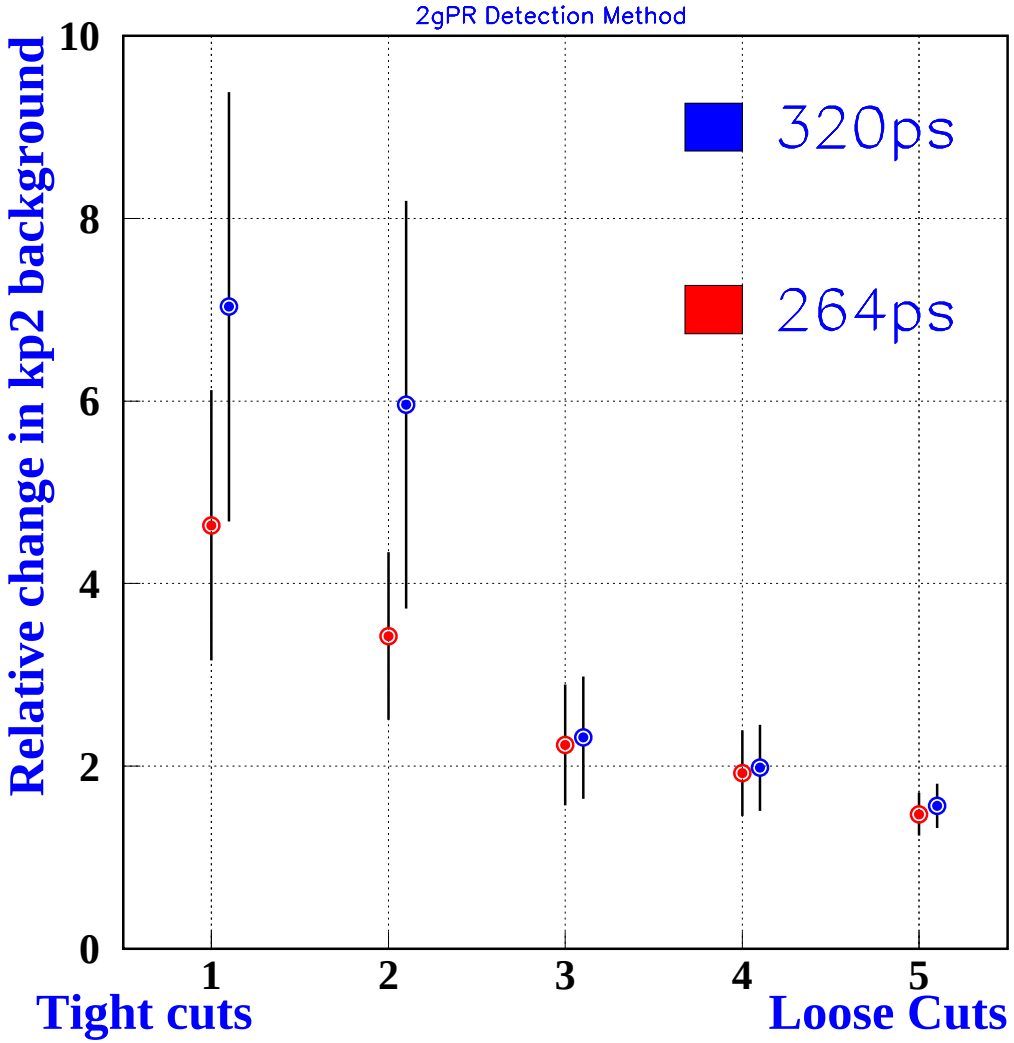

Relative $K_L^0 \rightarrow \pi^0\pi^0$ background rate if kinematic cuts optimized for a microbunch width of 200 ps are applied to FastMC data with microbunch widths of 264 ps and 320 ps.

Optimal sensitivity requires an accurately measured, stable microbunch width.

Deadtime/losses due to neutrons

The rates in the CPV and PV (including the PR and CAL and excluding the beam catcher) due to neutron halo interactions was estimated with a GEANT3 simulation of the KOPIO neutral beam to be 1 MHz and 1.5 MHz, respectively, at $N_K = 4.32\ \mathrm{K_L^0}$ exiting the spoiler per microbunch. The random losses in the beam catcher due to neutron interactions is estimated from GEANT3 studies at $N_K = 2.10$ to be 4.6%.

At the optimum spill length, we have $N_K = 2.02$, the loss due to halo neutrons is 0.014 and the loss due to neutron beam interactions in the catcher is 0.045. By contrast, the loss due to stopped muons is 0.115 and the loss due to $\mathrm{K_L^0}$ decays in the same microbunch is 0.376.

Effect of magnetic fringe fields on background rejection

The primary effect of non-zero magnetic fields on background suppression is that the path length of charged particles from the $\mathbf{K_L^0}$ decay point to the CPV will be drastically increased so that the charged particles would fall outside of any reasonable timing window. Timing windows of $\mathbf{-4 < \Delta < 8\ ns}$ have been shown to give good background suppression where $\mathbf{\Delta \equiv TOF - \mathit{d}/\mathit{c}}$, $\mathbf{TOF}$ is the measured time-of-flight of the charged particle from the $\mathbf{K_L^0}$ decay vertex and $\boldsymbol{d}$ is the distance from the decay vertex to the CPV impact position.

We expect magnetic fringe fields in the decay region from the D3 and D4 magnets. Studies indicate that mirror plates on the downstream end of D3 and the upstream end of D4 result in fringe fields of $\mathbf{\sim 50\ Gauss}$ at the upstream and downstream ends of decay region. If D3 and D4 have opposite polarities, the net field in the decay region is further reduced.

Effect of magnetic fringe fields on background rejection (continued)

A GEANT3 study of the effect of fringe fields on low momentum charged tracks was performed. For the purpose of the study, the field was assumed to vary linearly from $\vec{B} = (-50, 0, 0)$ at the upstream end of the decay region to $\vec{B} = (50, 0, 0)$ at the downstream end of the decay region. The demise of the $e^{\pm}$ from 5000 $\mathbf{K^0_L} \rightarrow \mathbf{K^{\mp}} e^{\pm} \nu$ decays was investigated as $\mathbf{K^0_L}$ beta decays provided a convenient way to get a sample of low momentum charged tracks distributed over the beam envelope.

Effect of magnetic fringe fields on background rejection (continued)

For $p > 3\ \mathrm{MeV}/c$, all $e^{\pm}$ struck the CPV with $\Delta < 5$ ns. For the 2279 $e^{\pm}$ with $p < 3\ \mathrm{MeV}/c$, 186 looped in the field until GEANT3 abandonned tracking and 55 others struck the CPV with $\Delta > 5$ ns. The "unveto-able" fraction of particles with $p < 3\ \mathrm{MeV}/c$ is $U = (186 + 55)/2279 = 0.11 \pm 0.01$.

From a FastMC study of the $\mathrm{K_L^0} \to \pi^+\pi^-\pi^0$, $\mathrm{K_L^0} \to \pi^{\pm}e^{\mp}\nu\gamma$ and $\mathrm{K_L^0} \to \pi^0\pi^{\pm}e^{\mp}\nu$(Ke4), only Ke4 produces any charged particles with $p < 3\ \mathrm{MeV}/c$ and the fraction of charged particles with $p < 3\ \mathrm{MeV}/c$ is $f(p < 3) = (3.6 \pm 0.8) \times 10^{-4}$.

The rate r of Ke4 relative to signal can be estimated as

$$\mathcal{B}(\mathrm{Ke4}) \times f(p < 3) \times \bar{\epsilon} \times U \ / \ \mathcal{B}(\mathrm{Kpnn}) = r$$

$$5.2 \cdot 10^{-5} \times 3.6 \cdot 10^{-4} \times 8.3 \cdot 10^{-6} \times 0.11 \ / \ 3 \cdot 10^{-11} = 5.7 \cdot 10^{-4}$$

where $\bar{\epsilon}$ is the veto inefficiency of the other charged particle and is estimated as $\sqrt{< \bar{\epsilon}_{\pi^+} \times \bar{\epsilon}_{\pi^-} >}$ evaluated for $K_L^0 \to \pi^+\pi^-\pi^0$ decays. A very pessimistic estimate of $\bar{\epsilon} = \max(\bar{\epsilon}_{\pi^-}) < 2 \times 10^{-4}$ yields $r < 0.014$.

Variations to baseline detector

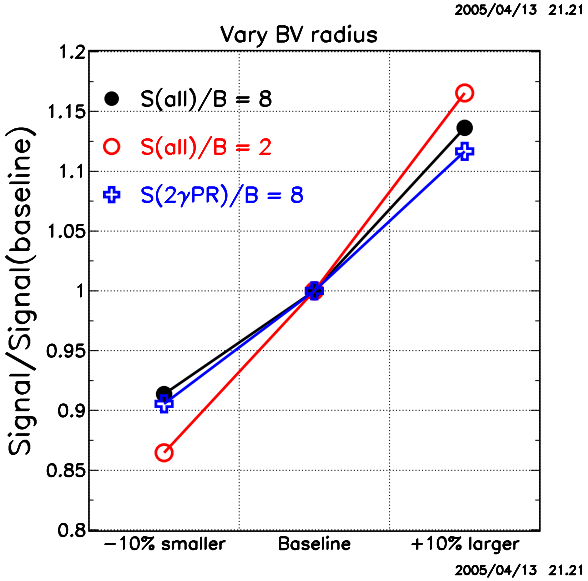

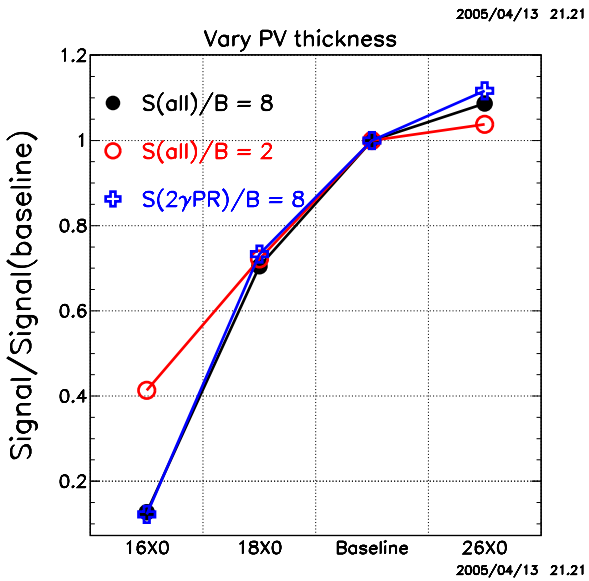

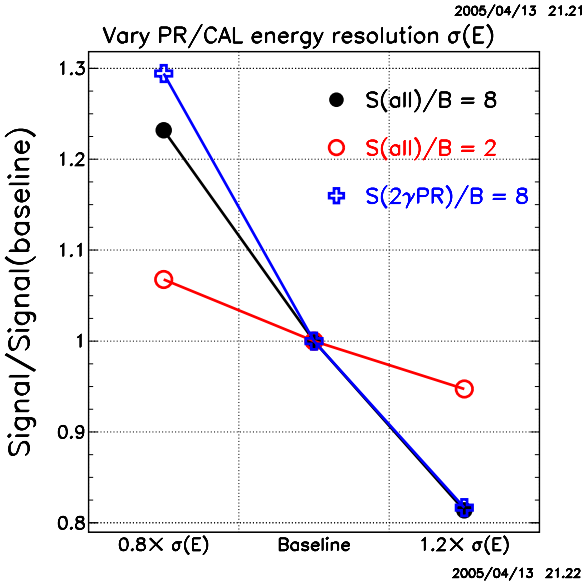

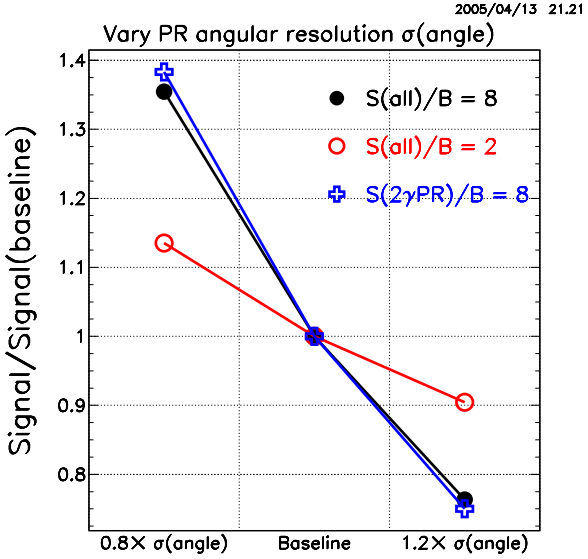

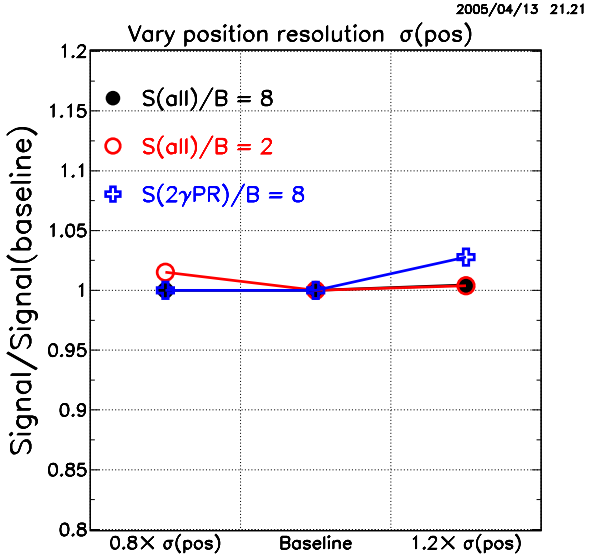

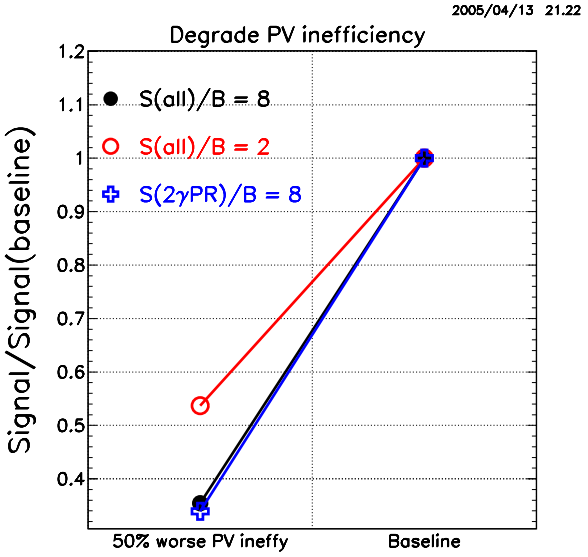

Variations to baseline detector (continued)

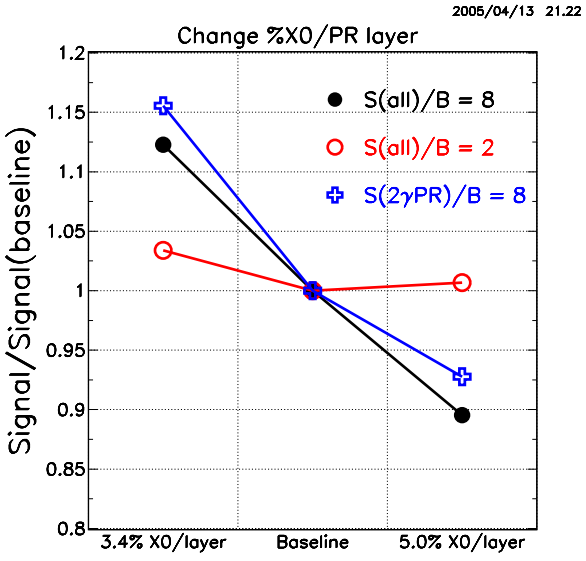

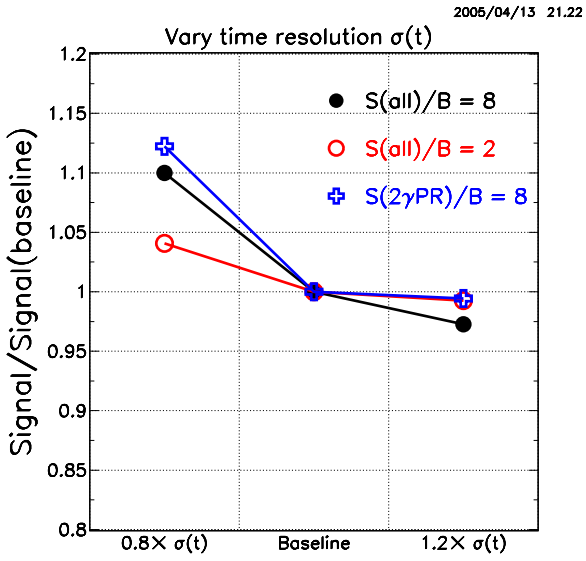

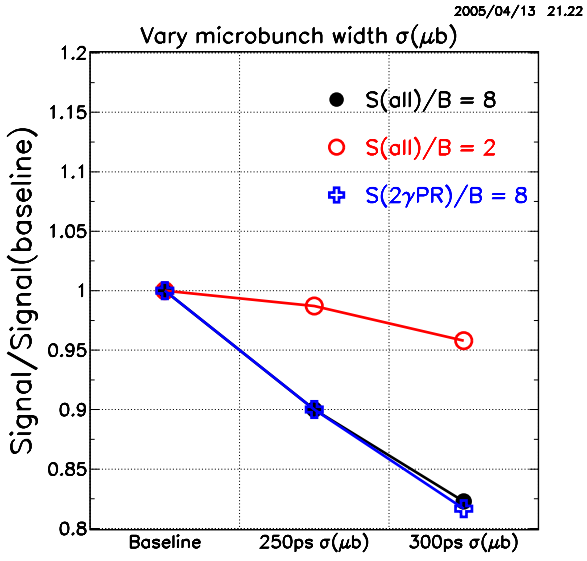

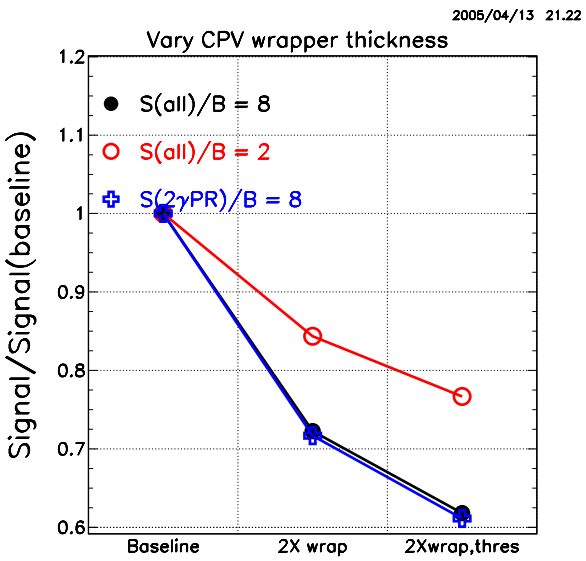

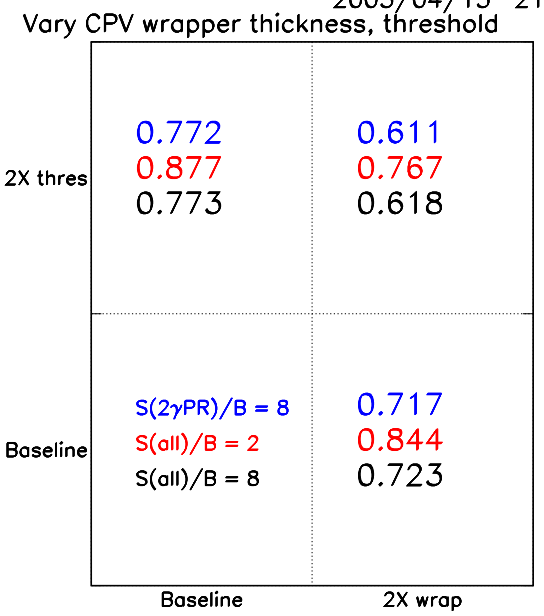

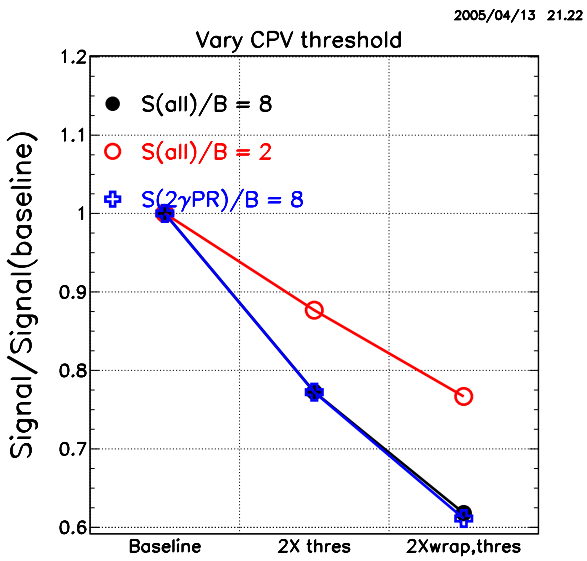

Veto detector studies

1. Effect of catcher double-pulse resolution
2. Rates compared to infinite PV and CV gates
3. Effect of position of CV in decay region
   - "far" position - veto lines inner wall of decay region
   - "near" position - veto has half-dimensions $\mathbf{111cm} \times \mathbf{50}$ cm

Effect of catcher double-pulse resolution (δt)

Catcher would be blind if γ from $\mathbf{K_L^0}$ arrives too close in time to γ from target produced by proton beam ("γ flash").

Time of γ at catcher from $\mathbf{K_L^0}$ is $t_c = t_K + d/c$ where d is distance from $\mathbf{K_L^0}$ decay to catcher. Approximate $d \approx z_{\mathbf{catcher}} - z_K \equiv z_c - z_K$ where $z_{\mathbf{catcher}}$ is US end of catcher.

Time of γ flash at catcher is $t_f = z_c/c$, so arrival time difference is
$\delta t = t_k - t_f = t_k + (z_c - z_K)/c - z_k/c = t_k - z_k/c = t_k(1 - \beta_z)$.

The δt cut is effectively a high momentum cut and removes $\mathbf{K_L^0}$ for which we otherwise have the best veto efficiency.

Next page shows momentum bite as a function of a cut on δt.

Effect of catcher double-pulse resolution

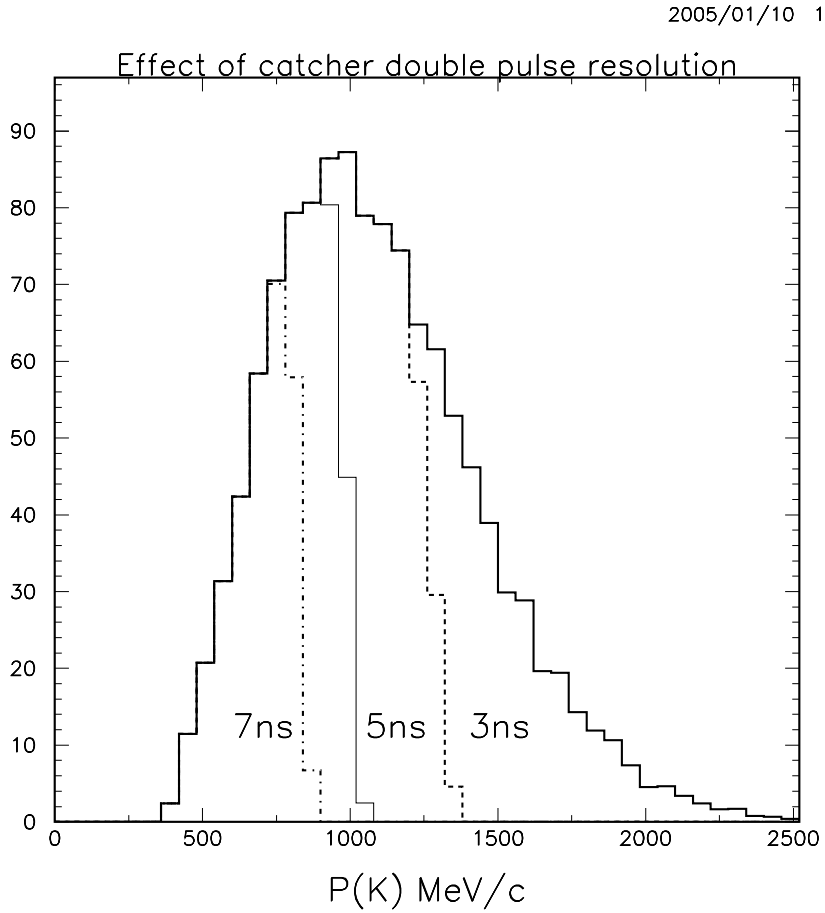

To recover the events ($P(K_L^0) > 1300$ MeV/c) when the catcher is blind, we make a kinematic fit using the Kp2 hypothesis and calculate the position of the missed photon at the catcher. A cut with 50% acceptance suppresses Kp2 background by 20×; the events can be recovered without reducing S/B.

A more restrictive catcher veto algorithm with ~ 0.05 inefficiency would recover all events without reducing S/B.

Rates with veto gates, 2γPR detection mode

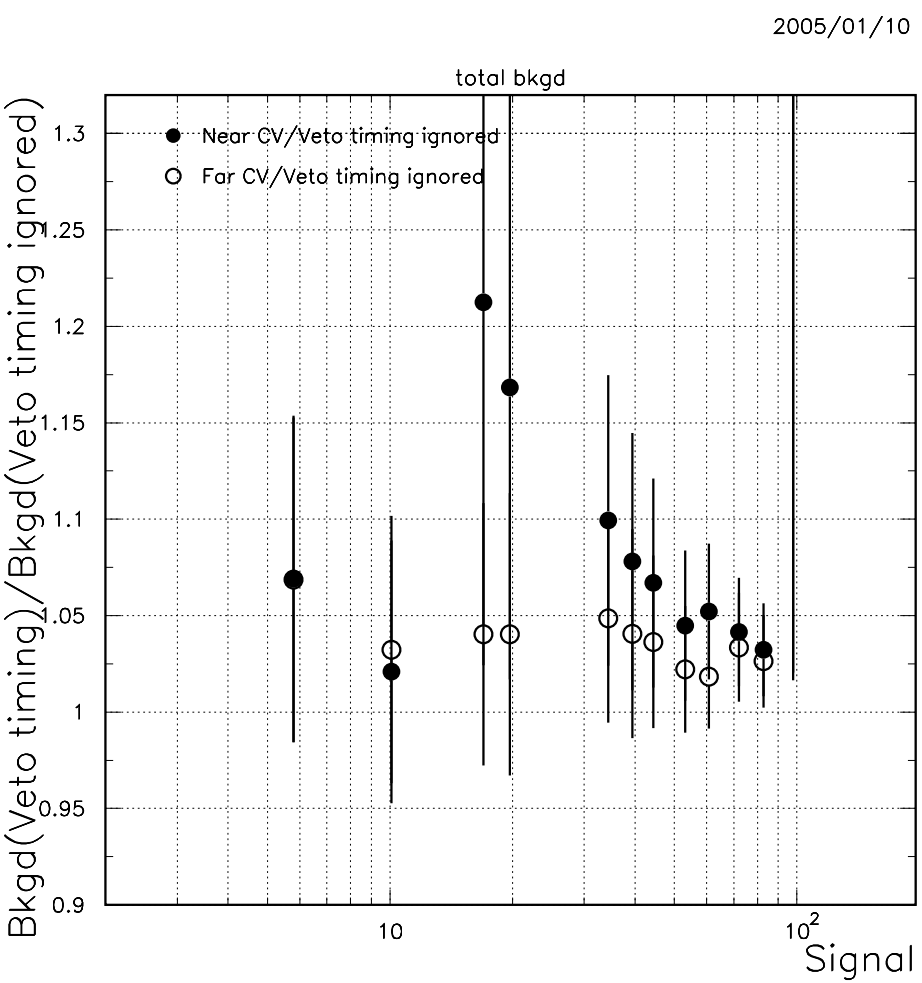

Background rate with/without veto timing.

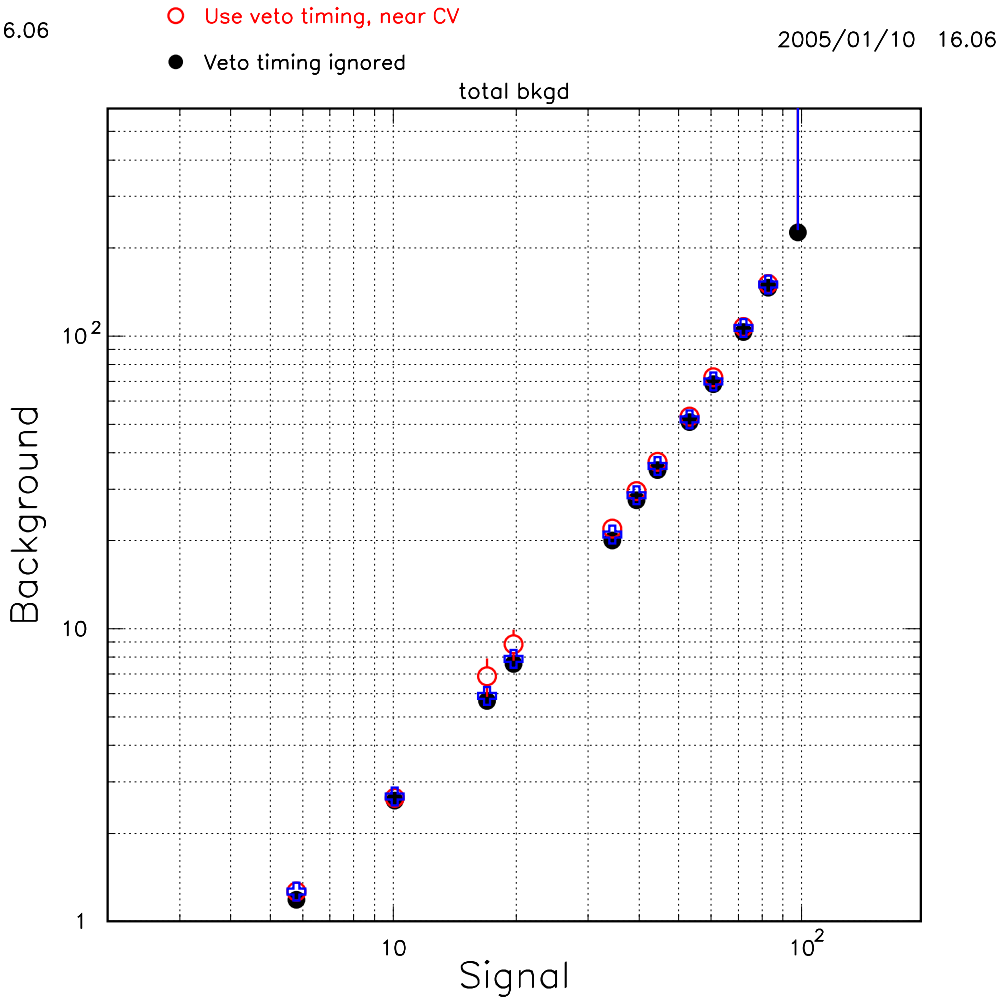

B *vs* S with & without veto timing and CV at near, far positions.